Energy Conversion and Management: X 30 (2026) 101819

Contents lists available at ScienceDirect

Energy Conversion and Management: X

journal homepage: www.sciencedirect.com/journal/energy-conversion-and-management-x

Efficient contract and regulation design for district energy systems using multi-agent modeling

Maximilian Hoffmann [b,e,*,1], Frieder Borggrefe [a], Detlef Stolten [b,c,e], Aaron Praktiknjo [a,d,**,2]

[a] RWTH Aachen University, Institute for Future Energy Consumer Needs and Behavior (FCN), Mathieustr. 10, 52074 Aachen, Germany
[b] Forschungszentrum Jülich GmbH, Institute of Climate and Energy Systems – Jülich Systems Analysis (ICE-2), 52425 Jülich, Germany
[c] RWTH Aachen University, Chair for Fuel Cells, Faculty of Mechanical Engineering, 52062 Aachen, Germany
[d] JARA-ENERGY, Jülich Aachen Research Alliance, 52074 Aachen, Germany
[e] JARA-ENERGY, Jülich Aachen Research Alliance, 52425 Jülich, Germany

ARTICLE INFO

Keywords:
Fifth-generation district heating and cooling
Energy system models
Multi-agent modeling
Bidirectional heating networks
Energy communities

ABSTRACT

Fifth-generation district heating and cooling (5GDHC) networks offer high energy efficiency, bidirectional thermal flows, and seamless integration of renewables and waste heat. However, their decentralized nature creates complex interactions between consumers and providers, particularly under fixed-price contracts.

This study evaluates how business models, pricing strategies, and regulatory measures affect such interactions in a real-world 5GDHC system in Hassel, Germany. A traditional energy system optimization model is extended into a discretized Stackelberg pricing game, capturing strategic price-setting by the provider and cost-minimizing behavior of 51 consumers. Unlike previous work that addresses technical design, stakeholder behavior, or policy separately, this approach integrates strategic interaction and regulation to quantify incentive misalignments, welfare losses, and emissions.

Results indicate that constant-price contracts can increase system-wide annualized costs by 8–18% relative to the social welfare optimum, measured using a new incentive alignment suboptimality metric. Combining CO_2 taxes (100 €/t) with investment subsidies (25%) effectively reduces both welfare losses and emissions, offering scalable insights for policy and utility design of future-ready district energy markets.

Introduction

The decarbonization of the residential sector is a key milestone on the path toward a climate-neutral energy system, as stipulated by international agreements such as the Kyoto Protocol [1] and the Paris Climate Agreement [2] to stay well below 2 °C of global warming. Yet, the heating sector is shaped by fragmented decision-making: energy consumption and investment choices are typically made by individual households, influenced by prices, regulations, and behavioral factors. This reality contrasts with the assumptions of many energy system models, which often neglect actor-specific objectives and constraints, which have been shown to play a crucial role in shaping energy system outcomes [3].

At the same time, the increasing complexity of modern energy systems, driven by higher shares of variable renewable energy, sector coupling, and emerging technologies, requires advanced planning tools, such as cost-minimizing bottom-up energy system models [4]. These models have proven effective for energy transition studies at local [5–9], regional [10], national [11–13] and international scales [14,15]. However, they often assume central planning which minimizes total system costs, without considering the interaction of diverse stakeholders with conflicting incentives.

To address this gap, this study proposes a multi-agent modeling approach based on a real-world 5th-generation district heating and cooling (5GDHC) system currently under development in Hassel, Germany. For that purpose, a traditional energy system optimization model is transformed into a discretized Stackelberg pricing game to reflect the hierarchical interaction between a price-setting energy provider and

* Corresponding author at: Forschungszentrum Jülich GmbH, Institute of Climate and Energy Systems – Jülich Systems Analysis (ICE-2), 52425 Jülich, Germany.
** Corresponding author at: RWTH Aachen University, Institute for Future Energy Consumer Needs and Behavior (FCN), Mathieustr. 10, 52074 Aachen.
E-mail addresses: max.hoffmann@fz-juelich.de (M. Hoffmann), apraktiknjo@eonerc.rwth-aachen.de (A. Praktiknjo).
[1] ORCID: https://orcid.org/0000-0003-1232-8110.
[2] ORCID: https://orcid.org/0000-0002-2151-4241.

https://doi.org/10.1016/j.ecmx.2026.101819
Received 7 January 2026; Received in revised form 22 February 2026; Accepted 2 April 2026
Available online 8 April 2026

price-taking consumers. In this setting, the energy consumers are represented as decision-making agents that minimize their respective total annualized costs in response to the energy provider's price signals, while the energy provider constitutes an additional agent optimizing its own system under the constraint of satisfying all aggregated consumer demands. Furthermore, this work assesses the role of regulatory interventions, namely CO_2 taxes and investment subsidies, in improving incentive alignment and reducing emissions.

Thereby, the following research questions are addressed:

1. How do multi-agent energy system models differ from traditional central-planner models in terms of cost, self-consumption, and coordination efficiency?
2. What impact do fixed-price contracts have on consumer investment behavior, system costs, and CO_2 emissions? Can regulatory instruments like price ceilings improve outcomes?
3. How can regulation align incentives between decentralized actors? Which combinations of taxes and subsidies are most effective in reducing welfare losses and emissions?

The novelty of this study lies in integrating strategic interaction and regulation within a multi-agent optimization framework for a real-world 5GDHC district. Unlike existing studies that focus on optimal technical design, stakeholder interaction, or policy analysis separately, this work combines a discretized Stackelberg pricing game with regulatory modeling to quantify incentive misalignments between stakeholders, as well as associated welfare losses and emission outcomes in decentralized heating systems.

State of the art

The following section reviews the current state of the art in optimizing 5GDHC networks, modeling diverging stakeholder interests in energy systems and markets, and representing regulatory frameworks in Subsections 2.1 – 2.3, respectively, highlighting that while advanced mathematical approaches exist for each of these areas individually, their combined optimization has rarely been addressed.

Fifth-generation district heating and cooling (5GDHC)

Heating accounts for a major share of energy demand in the residential sector. With the growing share of variable renewable energy sources, system flexibility becomes essential. Simultaneously, advanced storage [8,16,17] and heating technologies are driven by rapid technological learning [18]. Therefore, they are indispensable for the transition to greenhouse gas neutrality [19] and for limiting future heating and electricity costs [20].

For district heating, a clear trend toward lower network temperature levels can be observed [21]. While first- to third-generation systems typically operate at >70 °C and are predominantly fossil-fueled [22], the emerging fifth-generation district heating and cooling (5GDHC) systems operate between 5 °C and 40 °C [6]. According to Buffa et al. [23], these networks are defined as:

- Operating at temperatures too low for direct space heating
- Covering heating and cooling demands simultaneously using shared pipelines

These low-temperature systems offer a range of advantages. They allow the integration of various low-grade heat sources [21], such as waste heat from data centers [24] and, in particular, from buildings, significantly improving overall system efficiency [19,25].

The advantages of using lower temperatures for district heating are manifold: lower temperature levels enable the integration of more potential technologies as heat sources or sinks. Among these is waste heat from data centers [24], and, predominantly, from buildings, which is a key to higher system efficiencies [19,25]. Low temperature networks also allow for simultaneous heating and cooling by obtaining the necessary temperature levels by heat pumps or compression chillers on the respective demand side. The most important advantages of fifth-generation district heating and cooling networks according to Wirtz [26] are a single low-cost network for heating and cooling, low heat losses without the necessity of insolation, direct use of low-grade waste heat including ambient-temperature heat sources such as air and rivers, and high flexibility with user-specific temperature levels.

In the literature, 5GDHC systems are referred to using a variety of terms, reflecting slightly different emphases in scope and design. These include "bidirectional low-temperature networks" [5,21,27–33], "thermal source networks" [34–39], "cold district heating networks" [40,41], "anergy grids" [42–44], "balanced energy networks" [45], and "low-temperature district heating and cooling" [46–50]. Despite terminological variation, they share the already stated features. Because "fifth-generation district heating and cooling (5GDHC)" is the most frequently used label in recent peer-reviewed literature [6,22,23,30,51–77], it is adopted throughout this study. An overview of terminology and recent publication trends is provided in Table 4 in Appendix A.1.

Diverging stakeholder interests

Most bottom-up, optimization-based energy system models aim to minimize total system costs from a central planning perspective. They do not represent different market participants or the contractual structures that govern their interactions. As such, they neglect the objectives and behavioral responses of market participants based on their individual costs and revenues.

In reality, however, many energy-related interactions resemble Stackelberg competition [78]. In such hierarchical settings, a first mover, which is typically an energy provider with price- or quantity-setting power, maximizes its own objective by anticipating how other actors (e.g., consumers) will respond to its decisions [79]. This naturally leads to bilevel optimization problems, where the upper-level problem (the leader's objective) is constrained by the optimal response of the lower-level problem(s) (the followers' behavior) [78].

If the lower-level problems are convex and fulfill Slater's regularity condition, they can be reformulated using the Karush-Kuhn-Tucker (KKT) conditions. In that case, KKT conditions provide necessary and sufficient conditions for optimality. By embedding the KKT conditions of the lower-level problems into the upper-level problem, the bilevel problem can be converted into a single-level one [78,80]. However, because the KKT formulation includes complementarity constraints, the resulting single-level problem becomes bilinear. To make the model solvable with standard mixed-integer programming tools, these bilinear constraints are often reformulated using big-M transformations [81], resulting in a mixed-integer linear program (MILP).

In practice, these models, also referred to as mathematical programs with equilibrium constraints (MPECs), are rare in energy system modeling [78]. This is often due to either non-convexity or complexity of the lower-level problems, or a modeling focus on system-wide optima, rather than decision-making f market participants.

Most of the few bilevel energy system models found in the literature focus on unit commitment or market modeling rather than capacity expansion, as shown in Table 1.

The examples in Table 1 either involve only one lower-level problem, or do not solve the bilevel model via KKT-based transformation. In contrast, district heating systems include few providers but dozens of individual consumers, each with individual objective functions. Embedding KKT conditions for every consumer into the provider's upper-level problem would generate a large number of bilinear or big-M constraints, significantly increasing computational complexity.

Therefore, the bilevel problem is decomposed by pre-solving consumer responses to a discrete set of possible contract inputs instead. This leads to a discretized Stackelberg model, which is computationally

Table 1
Excerpt of literature on bilevel energy system models relevant to this study.

Author	Year	Reference	Application case	Upper level	Lower level	Type	Bilevel solution approach
Li et al.	2019	[82]	Energy hub bidding for electricity and heating	Electricity and heating market bidding	Market clearing and contracting	Dispatch	KKT-based MPEC
Li et al.	2017	[83]	Coupled electricity and gas dispatch with P2G and G2P	Electricity dispatch with coal and wind	Allocation of a natural gas system	Dispatch	KKT-based MPEC
Hu et al.	2016	[84]	Economic energy dispatch under wind power uncertainty	Fuel and emission cost minimization	Minimization of the interval reduction of wind power output	Dispatch	Teaching–learning algorithm
Ju et al.	2016	[85]	Virtual power plant optimization	Income maximization of the virtual power plant	Operation cost minimization of a day-ahead schedule	Dispatch	Serial evaluation (non-KKT)
Škugor and Deur	2016	[86]	EV fleet charging for delivery services	Final State-of-Charge (SoC) optimization of individual EVs	Aggregate charging power is optimization	Dispatch	NSGA (upper level) + dynamic programming (lower level)
Feijoo and Das	2015	[87]	Emissions control in a microgrid	Microgrid operation	Linear electricity dispatch	Dispatch	KKT-based MPEC
Liu and Li	2015	[88]	Electric power dispatch and load control	Electricity generation and dispatch	Load control optimization	Dispatch	Non-dominated sorted genetic algorithm (NSGA-II)
Valinejad and Barforoushi	2015	[89]	Generation capacity expansion	Investor's profit maximization	Market clearing and social welfare optimization	Capacity expansion	KKT-based MPEC
Jenabi et al.	2013	[90]	Transmission and generation expansion planning	Transmission operator investment planning	Market clearing with multiple rival generation firms	Capacity expansion	KKT-based MPEC

tractable and better suited to the regulatory and strategic context of fifth-generation district heating and cooling systems. The implementation is detailed in Section 3.2.

Legal regulations

Legal regulations are a key driver of the energy transition. However, they vary widely across countries and are subject to frequent updates so that investments will likely face regulatory changes during their economic lifetimes [91]. Both factors hinder generally applicable modeling approaches. Yet, regulation is essential for aligning incentives among market participants and a prerequisite to transform the energy system into an efficient and sustainable one [92].

In Europe, for example, current legal debates focus on whether to extend third-party access rights, which are already applied to gas and electricity grids, to district heating networks, and under what conditions grid operators may be exempted [93]. Similarly, energy communities envisioning a joint district energy production and consumption is envisioned by the EU [94] but the implementation varies across member states [95,96]. This reflects a broader need to integrate legal dimensions into energy system modeling, especially in district energy systems.

Several studies have embedded regulatory mechanisms into residential energy system models. These include subsidies, taxes, grid tariffs, CO_2 restrictions, and feed-in remuneration schemes. Table 2 summarizes key examples from the literature.

Recently, the authors of this study investigated the impact of regulations on the transition of the German residential heating sector in a series of journal articles [104], conference presentations [105,106] and posters [107,108]. They conclude that the current German regulation could impede the concept of energy communities [107] and the transition of the heating sector itself [104].

Although regulatory modeling approaches differ significantly across countries, time periods, and technology scopes, most can be broadly categorized into capital expenditure (CAPEX) and operational expenditure (OPEX) schemes. CAPEX schemes typically include investment subsidies for clean technologies, while OPEX schemes affect commodity flows, either through penalties such as CO_2 taxes or incentives like feed-in tariffs for renewable energy. Accordingly, this study considers basic investment subsidies, CO_2 taxes on heat and electricity, and feed-in remuneration, as detailed in Subsection 3.3.

Methodology

The following subsections introduce the case study as a traditional

Table 2
Excerpt of studies considering regulation schemes in the residential energy sector.

Author	Year	Reference	Application case	Country	Bilevel solution approach
Pina et al.	2021	[91]	Hospital in Campinas	Brazil	Power exchange tariffs, commodity subsidies and surcharges, renewable investment subsidies, CO_2 bans
Benalcazar et al.	2020	[97]	Microgrid of a village with 90 households	Subtropical region, not specified	Cost and subsidy variations for RES (wind, PV) and distributed generation technologies
Pinto et al.	2020	[98]	Single and multi-family homes in Zaragoza	Spain	Self-consumption laws, feed-in tariffs
González-Mahecha et al.	2018	[99]	Municipal building system with PV, micro wind turbines, and battery storage in Lisbon	Portugal	Pricing schemes for feed-in tariffs
Renaldi et al.	2017	[100]	Residential heating system including heat pumps and thermal storage	UK	Operational heat pump subsidies via Renewable Heat Incentive (RHI)
Schütz et al.	2017	[101]	Residential buildings	Germany	PV feed-in limits (EEG), PV investment subsidies (KfW), remuneration for feed-in and self-consumption from CHPs (KWKG)
Harb et al.	2016	[102]	Heating systems in residential buildings for single- and multi-family houses, apartment buildings and a heating network	Germany	Above-market PV feed-in remuneration, gas tax exemptions for CHP
Lozano et al.	2010	[103]	CCHP system for 5000 apartments	Spain	Minimum self-consumption quotas for electricity from CHP

central-planner optimization model and describe how this model can be transformed into a discretized multi-agent one from both a theoretical and practical point of view. Finally, Subsection 3.3 describes how to consider different regulation schemes in both the central-planner and multi-agent models.

Case study and input data

This study focuses on one of four district energy systems being developed as part of the TransUrban.NRW project, an initiative aimed at demonstrating highly efficient renewable energy solutions in the residential sector of North Rhine-Westphalia, Germany [109]. The case modeled here refers to the "Stadtteilpark Hassel" in Gelsenkirchen, a district that integrates a fifth-generation district heating and cooling (5GDHC) network, thermal and electrical storage systems, and widespread rooftop photovoltaic (PV) installations. The buildings comply with modern insulation and heating standards, making the district a forward-looking example of future residential energy infrastructure. The layout includes 5 buildings, the consumer locations, and a centralized energy provider at location 36, as detailed in Fig. 1.

Fig. 2 outlines the modeled system structure. The energy provider and the 51 consumers are each equipped with its own set of technological options. Consumer energy demands include electricity, space heating (via radiators or floor heating), domestic hot water, and cooling. Each consumer can either purchase commodities from the provider or meet part of their demand autonomously. Heating options include three heat pumps: (1) a water-to-water heat pump that upgrades 5GDHC network heat from 35 °C to 55 °C to supply radiators and hot water, i.e., it uses water from the 5GDHC network to heat domestic hot water or water for radiator heating to 55 °C; (2) an air-to-water heat pump; and (3) a geothermal heat pump. The latter two use ambient air or ground temperature to feed heat into the 5GDHC network for use in floor heating or by the water-to-water unit. Thermal storage is available to buffer domestic hot water demand. Consumers can also install PV systems and batteries, allowing for local electricity generation and storage, and may sell surplus electricity to the provider.

On the provider side, technology options include ground-mounted PV and battery storage, air-to-water and geothermal heat pumps for feeding the 5GDHC network, and a compression chiller for meeting cooling demand. The provider may also purchase and sell electricity via the public grid, and import high-temperature district heat from a neighboring network, for which consumers incur additional costs. Access to this high-temperature district heating network, shown in red, was included as a purely comparative benchmark motivated by discussions with the industry partner, allowing the proposed 5GDHC concept, represented by orange and blue lines, to be evaluated against conventional district heating under identical boundary conditions. The high-temperature option is therefore not considered part of the baseline or recommended 5GDHC system design; instead, it is included to explore under which price configurations conventional district heating may become economically preferable to the 5GDHC network for specific heat demands, such as domestic hot water. Additional infrastructure costs associated with pipeline access are considered, while detailed hydraulic design aspects, including pipe diameter sizing, are intentionally excluded, as the focus of this work lies on techno-economic and incentive-related trade-offs rather than on detailed engineering design.

For simplicity, the 5GDHC network is modeled as two separate subcycles: one for low-temperature heating (~35 °C) and one for low-temperature cooling (~0 °C). Temperatures are not modeled explicitly; they are only used to calculate time-varying COPs of the heat pumps and the compression chiller over the course of a year as described in Appendix A.4. The model focuses solely on heat flows in kW exchanged between consumers and the energy provider within each subsystem. This approach reduces computational complexity and facilitates separation into consumer- and provider-side subsystems, avoiding highly interdependent constraints. While this simplification neglects heat losses along the line and limits the model's ability to capture how consumers' actions affect network temperatures, heat pump and compression chiller efficiencies, it facilitates model separation while still capturing basic network behavior.

Component costs are listed in Table 5 in Appendix A.2. An internal interest rate of 2% is assumed for consumers, consistent with the European Central Bank's medium-term inflation target [110], while the provider applies 8.5%, reflecting an average corporate weighted average cost of capital (WACC) across industries according to a current study by KPMG [111]. Although energy-sector WACC values are typically lower (5.2–7.4%) and technology-sector values higher (8.3–10.0%), the mean value was selected to represent the emerging and innovation-driven nature of 5GDHC investments. Since the 5GDHC network is modeled implicitly, infrastructure costs and losses are excluded. Two CO_2 accounting flows are tracked: one between consumers and the provider, and another between the provider and the external grids for electricity and high-temperature heat. These flows are calculated using emission factors and can be taxed accordingly. For electricity and high-temperature heat (HTH), emission factors of 390 g/kWh and 190 g/kWh were assumed, respectively, based on average values from recent

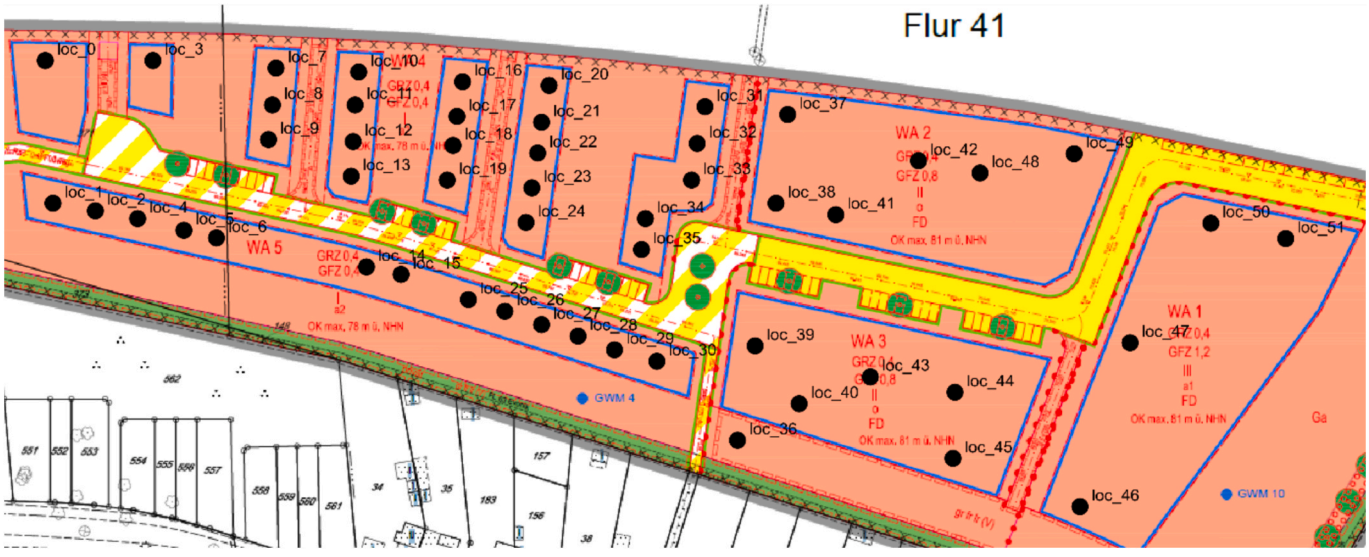

Fig. 1. Building locations in the residential district in Hassel and the location of the energy provider (location 36).

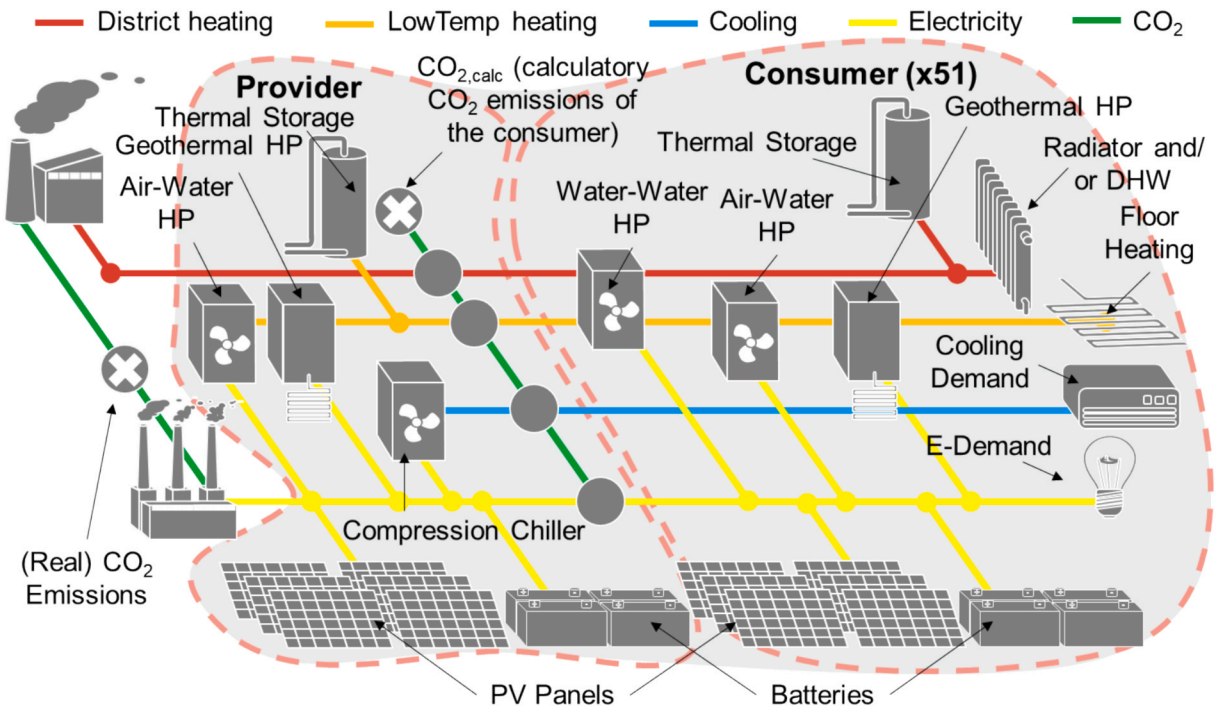

Fig. 2. Component options for the 51 consumers and the energy provider.

years in Germany [112,113]. For low-temperature heat (LTH) and cooling, emission factors are set to zero, as these are generated by CO_2-neutral heat pumps and compression chillers.

Each of the 51 consumer sites considers individual demand profiles and their simulation approach is described in detail in Appendix A.3. They include domestic hot water, space heating, cooling, electricity, and rooftop PV capacity factor time series for a potential on-site energy supply.

The initial formulation assumes central planning minimizing the total annualized system cost across all 51 energy consumers and the provider simultaneously. It also includes binary decisions, such as the choice between floor and radiator heating. All models—including central planning as well as the separate consumer and provider models presented in the following subsection—are formulated as mixed-integer linear programs (MILPs). They are implemented using the Python-based energy system modeling framework ETHOS.FINE [12,114] and solved with Gurobi.

To reduce computational complexity, temporal aggregation techniques [115–118] were applied. Specifically, ten typical days [117] were selected using a clustering algorithm that preserves the value distributions of the original time series [116], and keeps aggregation-induced distortion minimal. Other techniques, such as heuristic

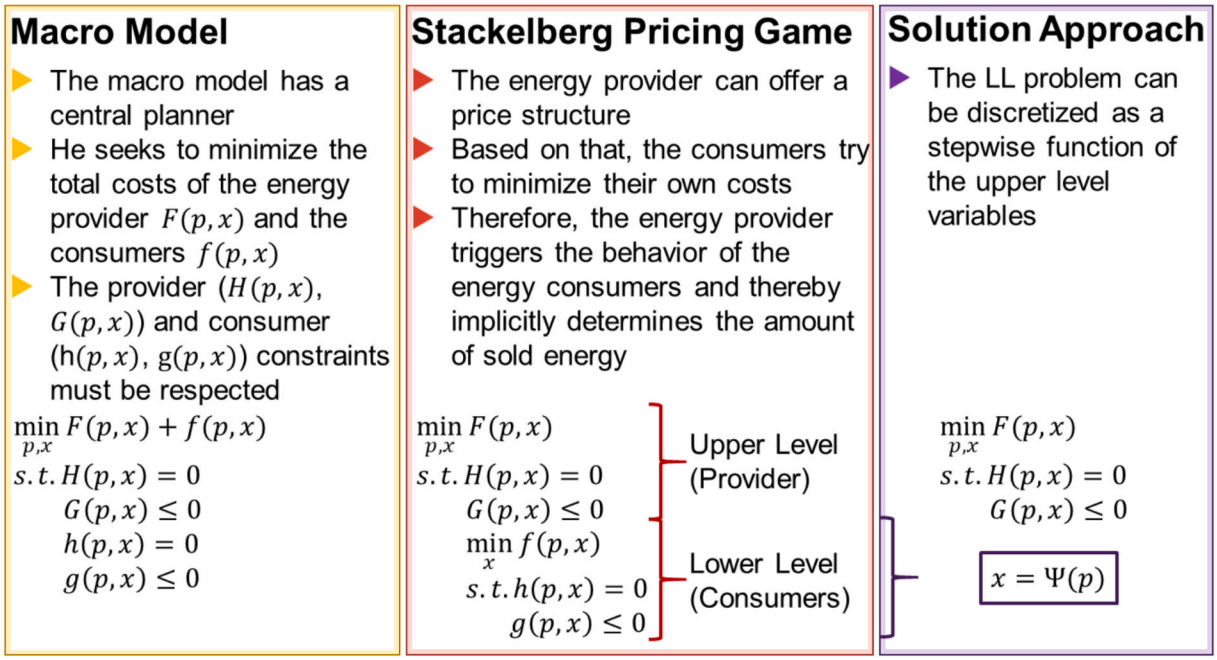

Fig. 3. Transformation from a central-planning into a discretized multi-agent energy system model.

fixation [119] or budget cutting [120], could also reduce complexity, particularly for binary decision variables. The decomposition into separate consumer and provider models is addressed in the following section.

Model separation and contract modeling

As introduced in Subsection 2.2, traditional bottom-up energy system models typically follow a central planning perspective. These models minimize a single objective function, usually total annualized cost or CO_2 emissions, across the entire system. In the context of this case study, this would imply that the energy provider and all consumers act in perfect coordination to jointly minimize the sum of their annualized costs, each applying their respective internal interest rates.

The left column of Fig. 3 illustrates this centralized model structure, in which x represents a vector of energy flows between the provider and consumers. p would denote a corresponding price vector although traditional models do not typically include explicit pricing. Instead, only commodity flows are optimized to minimize total system costs. Where dispatch models are used, market-clearing prices may be inferred ex post via shadow prices, but they are not part of the optimization variables.

However, if the energy provider possesses price-setting power, the model structure changes fundamentally. As shown in the center column of Fig. 3, the provider acts as a leader, setting price parameters to minimize its total annualized costs, reduced by the revenues from the consumers. Consumers, by contrast, act as price-takers: they treat the offered prices as fixed inputs and respond by adjusting their energy procurement strategies to minimize their own costs. This introduces a hierarchical interaction between the provider and consumers, a classic Stackelberg pricing game. According to Subsection 2.2, this results in a bilevel optimization problem that is difficult to solve directly, especially in systems with many heterogeneous consumers.

To maintain tractability, a discretized Stackelberg modeling approach is adopted, inspired by the method used by Sinha et al. [121]. This is illustrated in the right column of Fig. 3. The key idea is to replace the lower-level (consumer) optimization problems with a discrete mapping function $\Psi(p)$ that links each price vector p to the consumer reactions, represented by the demand vector x. This mapping is constructed by solving the consumer optimization models ex ante for a set of predefined price constellations. Importantly, the mapping function $\Psi(p)$ is neither continuous nor continuously differentiable in general. As a result, the upper-level provider optimization problem becomes non-convex and may exhibit multiple local optima.

In theory, the discrete Stackelberg game is then solved iteratively as follows:

1. Fix a price vector p
2. Solve all consumer models to obtain their demand responses
3. Aggregate demands and calculate revenues based on p
4. Optimize the provider model given these inputs
5. Iterate over alternative price vectors to improve profits for the provider

In practice, each of the 51 consumer subsystems illustrated in Fig. 4 is first solved for a fixed set of price combinations. For the present model, five prices could be varied: High-temperature heat (HTH), low-temperature heat (LTH), cooling, electricity, and electricity feed-in tariffs. However, due to the exponential growth in scenario space, and the central importance of LTH and electricity prices in consumer cost structures, the following analysis focuses on just these two dimensions, denoted p_1 and p_2 in Fig. 4.

Once the aggregated energy demands from all consumers $x = \Psi(p)$ have been computed for a given price vector, they are passed to the provider model, together with the corresponding price vector p, illustrated in Fig. 5. The resulting commodity-specific revenues, obtained by multiplying prices and quantities, define the provider's income, which is analyzed in detail in Subsection 4.1. The provider model then seeks to minimize system costs for providing the demanded energy and outputs the realizable profit for the given price vector, constituting a pointwise solution to the Stackelberg pricing game. The full mathematical formulation of both the consumer and provider models, as well as the mapping-based decomposition approach, is provided in Appendix A.4.

Regulation modeling

As discussed in Subsection 2.3, regulatory frameworks vary

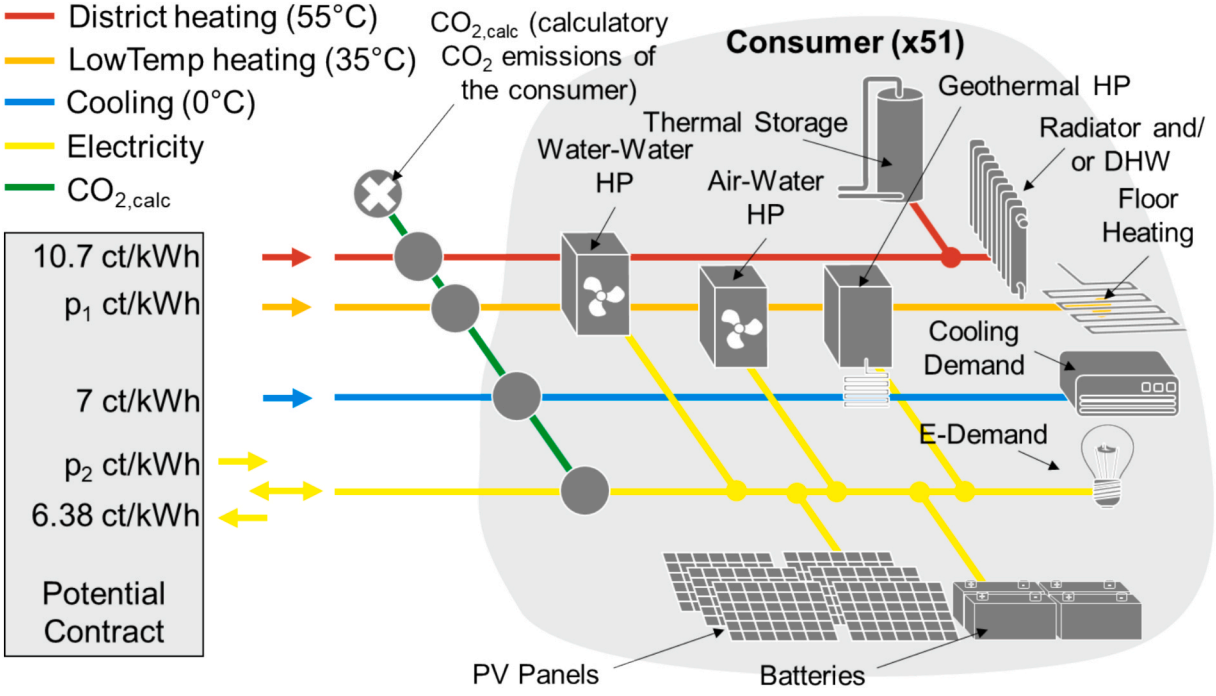

Fig. 4. The consumers' subsystems.

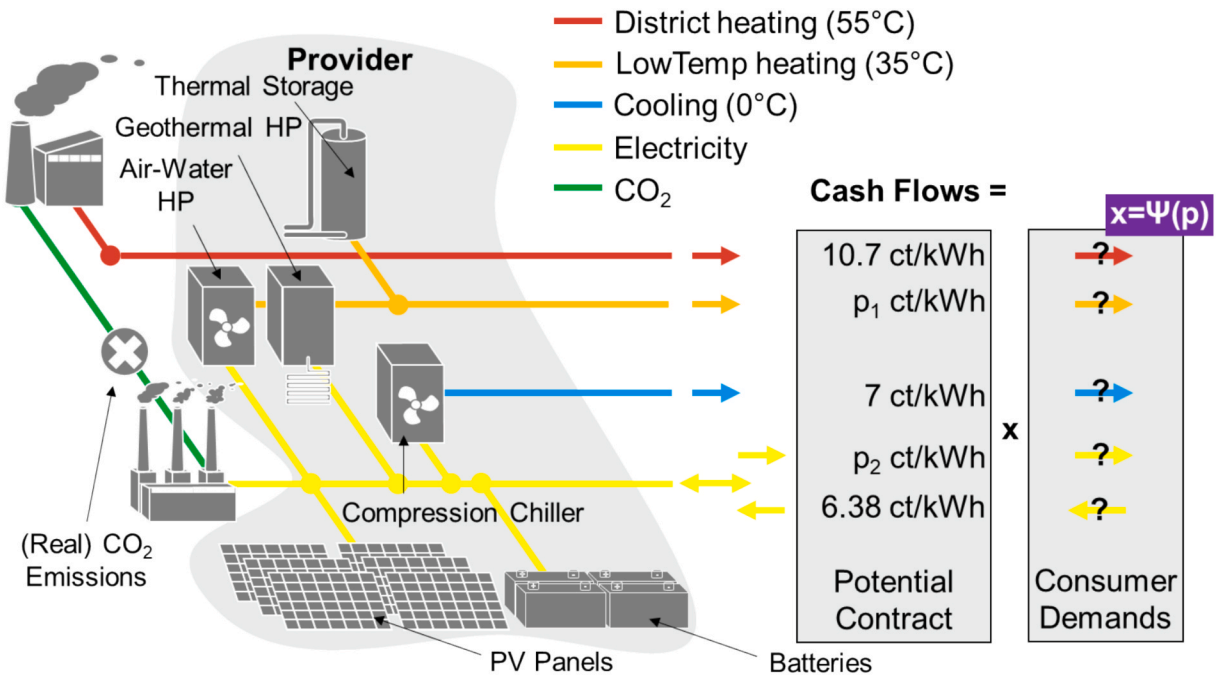

Fig. 5. The provider's subsystem.

significantly across countries and jurisdictions, making it challenging to model them generically. Nevertheless, to assess the fundamental effects of regulation on system outcomes, this study considers two widely applied policy instruments:

- An investment subsidy of 25% for carbon–neutral technologies
- A CO_2 tax of 100 €/t

These instruments are applied selectively to the provider, the consumers, or both. Fig. 6 visualizes the affected system components. The two instruments, each applicable independently to either party, can be freely combined, resulting in 16 regulatory constellations, summarized in Table 3. The scenarios range from a fully unregulated baseline (no subsidy, no tax), shown in the upper left cell of Table 3, to a fully regulated case where both parties are subject to both instruments ("Both for Both"), shown in the lower right cell of Table 3. For completeness, all other combinations are tested as well — for example, Run 7 describes the case in which the consumers receive a 25% investment subsidy on their components but are exempt from paying a CO_2 tax on their electricity and high-temperature heat (HTH) demand, while the energy

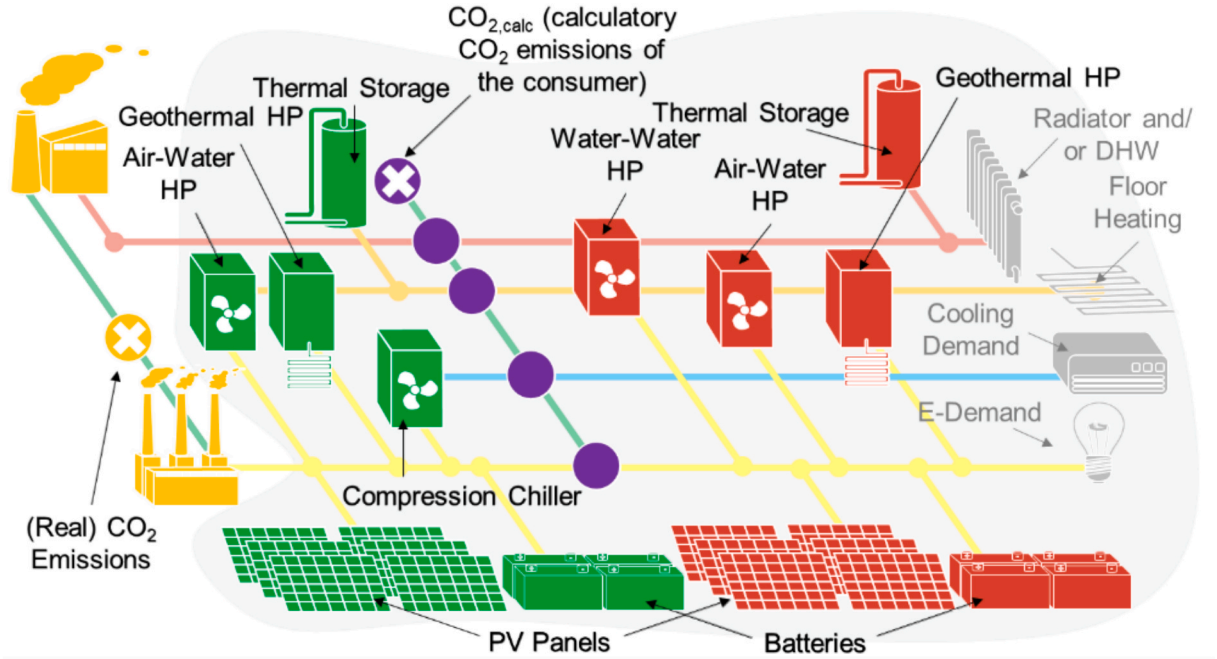

Fig. 6. System components subject to regulation measures. Red- and green-shaded technologies indicate investment subsidies for consumers and the provider, respectively. Violet and orange denote CO_2 taxation applied to the consumers' and provider's CO_2 balance, respectively. (For interpretation of the references to colour in this figure legend, the reader is referred to the web version of this article.)

Table 3
Regulation constellations obtained by cross-combining CO_2 taxes and subsidies for the consumers and provider.

Provider	Consumer	No Subsidy		Subsidy (−25% on Invest)	
		No CO_2 Tax	CO_2 Tax (100 €/t)	No CO_2 Tax	CO_2 Tax (100 €/t)
No Subsidy	No CO_2 Tax	Baseline	Run 2	Run 3	Run 4
	CO_2 Tax	Run 5	CO_2 Tax Both	Run 7	Run 8
Subsidy (−25% on Invest)	No CO_2 Tax	Run 9	Run 10	Subsidy Both	Run 12
	CO_2 Tax	Run 13	Run 14	Run 15	Both for Both

provider does not receive any investment subsidy and must pay a CO_2 tax of 100 €/tCO_2 for all imported electricity and HTH. In our model, double-counting of the CO_2 tax is possible, e.g., under the "Both for Both" constellation the consumer pays CO_2 tax on all electricity and HTH they request from the provider, and the provider in turn pays CO_2 tax on the electricity and HTH they import from upstream grids. In case of HTH, this is effectively doubling the CO_2 tax because the provider has no own generation technologies in place. While this does not perfectly reflect all current legal frameworks, which, in practice aim to avoid "double taxation" of the same emissions, the simplification was chosen in order to ensure consistent and comparable analysis across all constellations in this study.

While the investment subsidy is implemented as a direct rebate on component CAPEX, the carbon emission tax is modeled by introducing CO_2 as an additional commodity. This commodity is linked to other energy streams, as illustrated by the green lines in Fig. 6, and is priced through an additional term in the objective function. A detailed description of the regulatory modeling is provided in Appendix A.4.

The regulation schemes are implemented in both the central planning and the multi-agent/Stackelberg models described in the previous subsections. They allow us to analyze how different policy designs influence technology adoption, emissions, costs, and the alignment of decentralized decisions with system-wide optima. The outcomes of this analysis are presented in Subsection 4.2.

Results

This section presents the results for different contract price configurations between the energy provider and consumers, focusing on investment decisions, commodity use and stakeholder profits for different CO_2 tax and subsidization schemes.

Impact of contract structures

As described in Subsection 3.1, the demand profiles for each consumer were individually simulated, resulting in consumer-specific, cost-optimal technology setups that vary according to the selected electricity and low-temperature heat (LTH) prices. This variation is illustrated in Fig. 7, which displays the cost-optimal investment decisions of all consumers for a price of 30 ct/kWh for electricity and 10 ct/kWh for LTH. The selected prices represent the median of the price ranges investigated in the remainder of this work and are used to illustratively demonstrate how different price constellations lead to heterogeneous, consumer-specific system outcomes.

Notably, single-family and terraced houses in the western part of the district (locations 0–35 in Fig. 1) benefit from relatively large roof areas, enabling them to install PV panels to reduce electricity purchases and sell excess electricity. In contrast, electricity purchasing forms a larger share of total expenditures for apartment blocks in the eastern district (locations 36–51). Although apartment buildings also install PV, they tend to consume most of their own generation due to high demand and limited rooftop area per capita.

Differences also emerge in thermal energy supply. Smaller apartment blocks in the center use a mix of HTH for domestic hot water and LTH for space heating, similar to single-family and terraced homes. Larger apartment blocks in the east tend to avoid HTH, instead meeting their thermal needs with water–water heat pumps powered by LTH. These buildings are also large enough to cost-effectively invest in geothermal heat pumps. Across all buildings, battery sizes are closely correlated with PV capacity, aiming to increase self-consumption and benefit from the spread between the electricity purchase price (30 ct/kWh) and the feed-in tariff (6.38 ct/kWh). A detailed overview of the respective commodity costs and annualized expenditures for own system components for each consumer is provided in Appendix A.5.

Despite the unique configurations of each consumer, the district can be grouped into three distinct building types: single-family and terraced

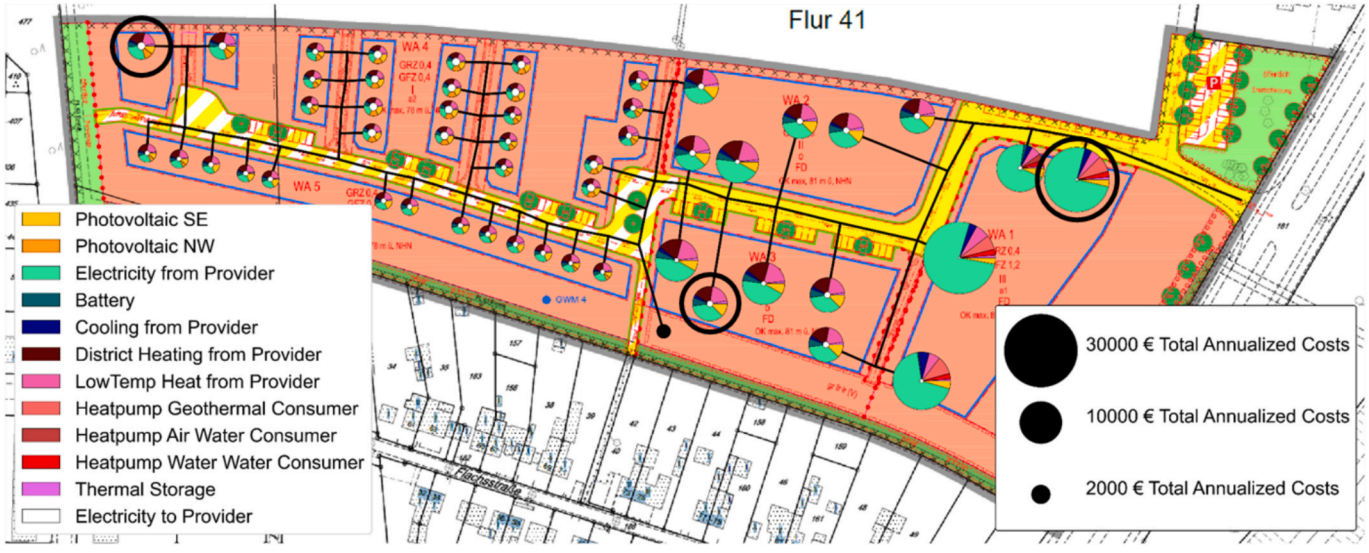

Fig. 7. Total annualized costs by technology for each consumer for 30 ct/kWh for electricity and 10 ct/kWh for low-temperature heat. The size of each pie chart reflects the magnitude of total annualized energy costs for the respective building. The segments indicate which share of these costs is spent on different technologies or commodities. Revenues from selling electricity to the provider are represented by the white circle at the center of each pie chart.

homes, medium-sized apartment blocks, and large apartment blocks. For clarity and brevity, the following analysis focuses on three representative buildings: location 0 (a large single-family house), location 40 (a medium-sized apartment block), and location 51 (a large apartment block). Terraced houses at locations 3–35 are excluded from further analysis because their investment response is limited: they switch from LTH to HTH when LTH prices exceed 16.5 ct/kWh, and their technology choices are not sensitive to electricity prices. As discussed in Appendix A.6, their lower energy demands compared to single-family houses do not justify more complex system configurations involving multiple heat pumps. Fig. 8 depicts the price-sensitive system configurations for the three representative buildings across a price plane spanning 20 to 40 ct/kWh for electricity and 0 to 20 ct/kWh for LTH.

At location 0, the cost-optimal design changes substantially across the price range. For low LTH prices, the building uses LTH for both space heating and domestic hot water. A water–water heat pump raises the LTH temperature to 55 °C for domestic hot water. As LTH prices increase and electricity remains relatively cheap, LTH is replaced by an air–water heat pump. At higher electricity prices, the air–water heat pump is retained for space heating, while HTH is used for domestic hot water. For moderate LTH and high electricity prices, the optimal solution involves using HTH for domestic hot water and LTH for space heating. While location 40 follows a similar logic, location 51 exhibits an additional configuration involving a geothermal heat pump. Though more expensive, this option is more efficient than an air–water heat pump and becomes viable under specific combinations of moderate to high electricity and LTH prices.

To understand the implications for the energy provider, Fig. 9 shows annual cash flows for LTH, electricity, HTH, and PV feed-in from the representative buildings. Each cash flow is computed as the product of the respective commodity price and annual demand. PV feed-in cash flows are negative for the provider, as they represent a cost and a corresponding revenue stream for consumers. Cash flows for cooling are omitted, as consumers cannot meet cooling demand themselves, making it perfectly inelastic and linear in price.

Fig. 9a shows that annual LTH revenues increase steadily with price until reaching tipping points where demand drops abruptly due to consumer switching. For example, at location 0, LTH demand collapses when the price exceeds roughly 6 ct/kWh. These tipping points correspond to non-continuous shifts in the consumer reaction function $\Psi(p)$, which reflects the substitution of LTH by heat pumps or HTH. This behavior is consistent with empirical findings on energy demand elasticities [122]. Across all three locations, LTH is gradually replaced as its price rises. Initially used for both domestic hot water and space heating, LTH is limited to floor heating at medium prices and often eliminated entirely at higher prices. At location 51, a specific configuration emerges in which LTH is used in combination with a geothermal heat pump to supply space heating.

Fig. 9b demonstrates that electricity revenues depend on both electricity and LTH prices. This interdependence arises because the adoption of heat pumps, driven by LTH prices, influences electricity demand. Higher LTH prices lead to complex technology combinations, particularly in location 51, where the optimal system can include no heat pumps or a full set of air–water, water–water, and geothermal heat pumps, depending on price conditions. For the provider, these transitions create discontinuous revenue surfaces with multiple local optima.

Fig. 9c presents cash flows for HTH, which was assumed to have a fixed price. Despite this, the cash flow varies significantly due to price-driven changes in consumer behavior. Depending on LTH and electricity prices, HTH may not be used at all, may be used solely for domestic hot water, or may cover both thermal needs. The third case, HTH for both uses, is only viable at moderate to high price levels, such as electricity prices of 40 ct/kWh and LTH prices of 20 ct/kWh for location 0.

Fig. 9d depicts feed-in cash flows, which are defined as negative costs for the consumers and exhibit a pattern similar to the ones for electricity demand. These consumer revenues decrease with higher electricity prices, as consumers increase self-consumption. Feed-in also drops when heat pumps are used, as PV generation is redirected to supply heating. This relationship further illustrates how electricity and thermal technologies interact and influence energy flows in non-obvious ways.

Although the building-level cash flows are highly sensitive to price and exhibit discontinuities, aggregated results across the full district yield smoother functions. Fig. 10 presents these aggregate outcomes. The left panel shows total consumer profits, which decrease monotonically with price. Even when consumers shift technologies in response to price changes, these shifts only limit profit decreases; they

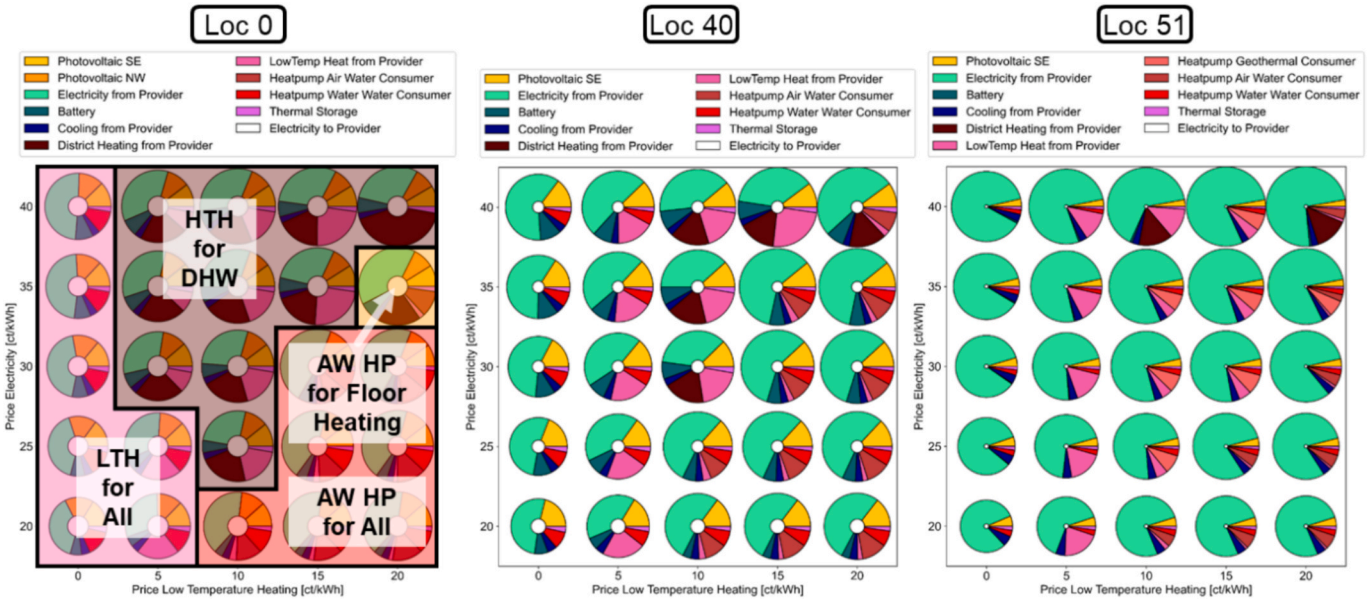

Fig. 8. Price-sensitivity of the total annualized costs by technology for the buildings at locations 0 (large single-family house), 40 (medium-sized apartment block), and 51 (large apartment block). The size of each pie chart reflects the magnitude of total annualized energy costs for the respective building, with the upper-right pie chart normalized to the same size across all subfigures. The segments indicate which share of these costs is spent on different technologies or commodities. Revenues from selling electricity to the provider are represented by the white circle at the center of each pie chart.

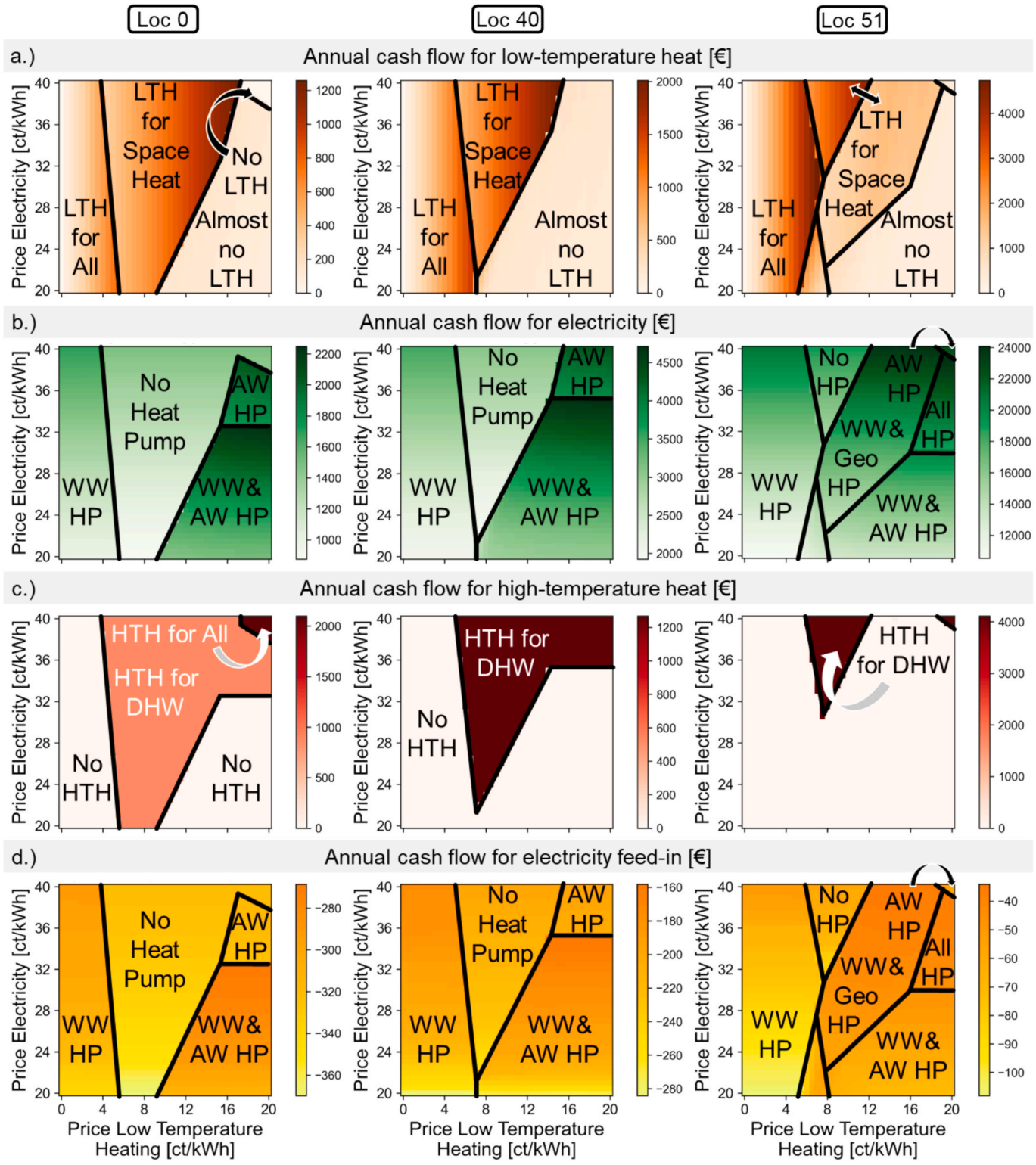

Fig. 9. The annual cash flows for LTH, electricity, HTH and electricity feed-in depending on the chosen price constellation at locations 0, 40, and 51.

cannot increase total profits. The center panel shows provider profits, which initially rise with LTH and electricity prices but decline beyond LTH prices of around 16.5 ct/kWh. This decline results from reduced LTH demand as consumers substitute heat pumps or HTH, which undercuts the provider's revenue.

As mentioned in Subsection 3.2, constant prices misalign incentives of the consumers and the provider, causing additional system costs. Accordingly, a price constellation can also be assessed by the additional costs it causes compared to the macroeconomic optimum, as defined in Eq. (1):

$$\Omega = \frac{\sum_{\text{consumers}}(\text{costs} - \text{revenues}) + \text{costs}_{\text{provider}} - \text{revenues}_{\text{provider}}}{\text{costs}_{\text{macro}} - \text{revenues}_{\text{macro}}} - 1 \tag{1}$$

This metric, the incentive alignment suboptimality, is shown in the right panel of Fig. 10. The results indicate that for LTH prices below

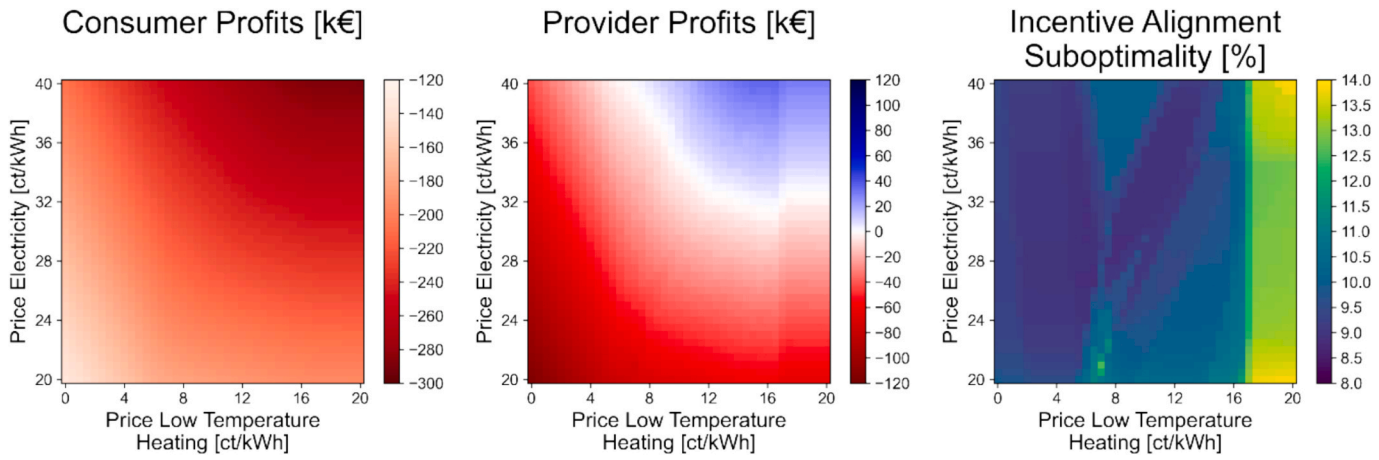

Fig. 10. Total annual profits of the consumers, energy provider, and the incentive alignment suboptimality, i.e. the cost-surplus of the multi-agent model compared to the central-planner model, as defined in Eq. (1).

approximately 6 ct/kWh, consumer and provider behavior aligns well with the centralized optimum, and the suboptimality remains at additional costs of at least 8.8%. However, for LTH prices above 16.5 ct/kWh, the deviation increases to values of up to 14%, highlighting the growing misalignment of incentives. These findings demonstrate that uncoordinated price-setting can lead to economically inefficient outcomes and indicate a potential role for regulatory interventions, such as price ceilings, to prevent excessive cost increases.

In summary, Fig. 10 shows that price structures strongly influence consumer costs, provider profits, and systemic efficiency. While well-chosen prices can lead to relatively efficient outcomes, poor alignment between stakeholder incentives can cause significant welfare losses. These results underscore the importance of regulatory design in shaping efficient and sustainable energy contracting environments.

Efficiency of the regulation schemes

This subsection analyzes the impact of the regulatory measures introduced in Subsection 3.3 on three key performance indicators: the deviation from the social welfare optimum, system-wide CO_2 emissions, and the financial balance of the regulation schemes themselves. These effects are assessed across the 16 regulatory constellations presented in Table 3, which result from the cross-combination of CO_2 taxation and investment subsidies for the energy provider and the consumers.

Fig. 11 illustrates the incentive alignment suboptimality for each configuration. The upper left cell represents the baseline case without any form of taxation or subsidization. Notably, the lowest deviation from the social welfare optimum is not achieved in this unregulated scenario, but rather in the constellation found in row 3, column 2, where the provider receives a 25% investment subsidy, and consumers face a CO_2 tax of 100 €/t. This result highlights that a well-designed regulatory scheme can help align decentralized decisions with macroeconomic efficiency, even in the presence of fixed commodity pricing.

A likely explanation for this outcome lies in the differing internal interest rates: the provider operates with a significantly higher internal rate (8.5%) than consumers (2%). Consequently, the annualized investment costs weigh more heavily in the provider's decision-making, making it more responsive to upfront cost reductions through subsidies. On the other hand, consumers react more strongly to CO_2 taxation than to subsidies. This can be attributed to their lower investment discounting, and to their ability to replace carbon-intensive HTH with low-emission LTH using water–water heat pumps, which is directly incentivized by CO_2 tax and a flexibility not available to the provider.

Fig. 12 presents the CO_2 emissions for the same regulatory configurations. Unlike the incentive alignment results, the most effective emission reduction occurs under the configurations in row 4, columns 3 and 4, where both consumers and the provider receive investment subsidies, and the provider is subject to CO_2 taxation. However, comparing these results to Fig. 11 reveals that the case in row 4, column 3, although favorable from an emissions standpoint, leads to a considerable deviation from the social welfare optimum. Therefore, the more balanced and preferable configuration appears in row 4, column 4, where all stakeholders are subject to both subsidization and taxation.

This dual-instrument approach, which incentivizes clean investment via subsidies and penalizes emissions through taxes, proves particularly effective. Yet, even under this configuration, some price constellations still lead to higher emissions due to persistent reliance on HTH. Thus, efficient price signals remain essential: effective regulation must be paired with economically rational pricing strategies to fully realize its decarbonization potential.

In addition to environmental and efficiency considerations, regulation also affects financial flows. Most real-world regulatory schemes involve a third-party actor, such as the state, that collects taxes and disburses subsidies. A well-balanced scheme minimizes the financial burden on any single party. To assess this aspect, Fig. 13 shows the total annualized costs and revenues in the central planning model under each regulatory configuration.

It becomes evident that configurations involving only taxation (row 2, column 2) or only subsidization (row 3, column 3) result in the largest deviations from the baseline in terms of total system costs. This is visually represented by the distance between the red dashed lines in Fig. 18. By contrast, the configurations previously identified as favorable, row 3, column 2 (from a welfare perspective) and row 4, column 4 (from an emissions perspective), result in relatively small cost deviations. Both schemes combine taxation and subsidization, leading to financially balanced outcomes for the regulator where state income from CO_2 taxes could offset the cost of technology support.

In summary, the two regulation schemes that perform best in terms of either incentive alignment or CO_2 reduction share a common feature: they employ a combined regulatory approach that includes both investment subsidies and CO_2 taxation. These combinations not only produce desirable environmental and macroeconomic outcomes but also offer fiscal neutrality, making them attractive from a policy implementation standpoint. A key insight from this analysis is that well-balanced, mixed regulatory instruments can enhance both system performance and political feasibility.

Discussion

The results provide clear answers on the initially stated questions, which are discussed in a political context in the following section. Furthermore, limitations of the current modeling approach are assessed

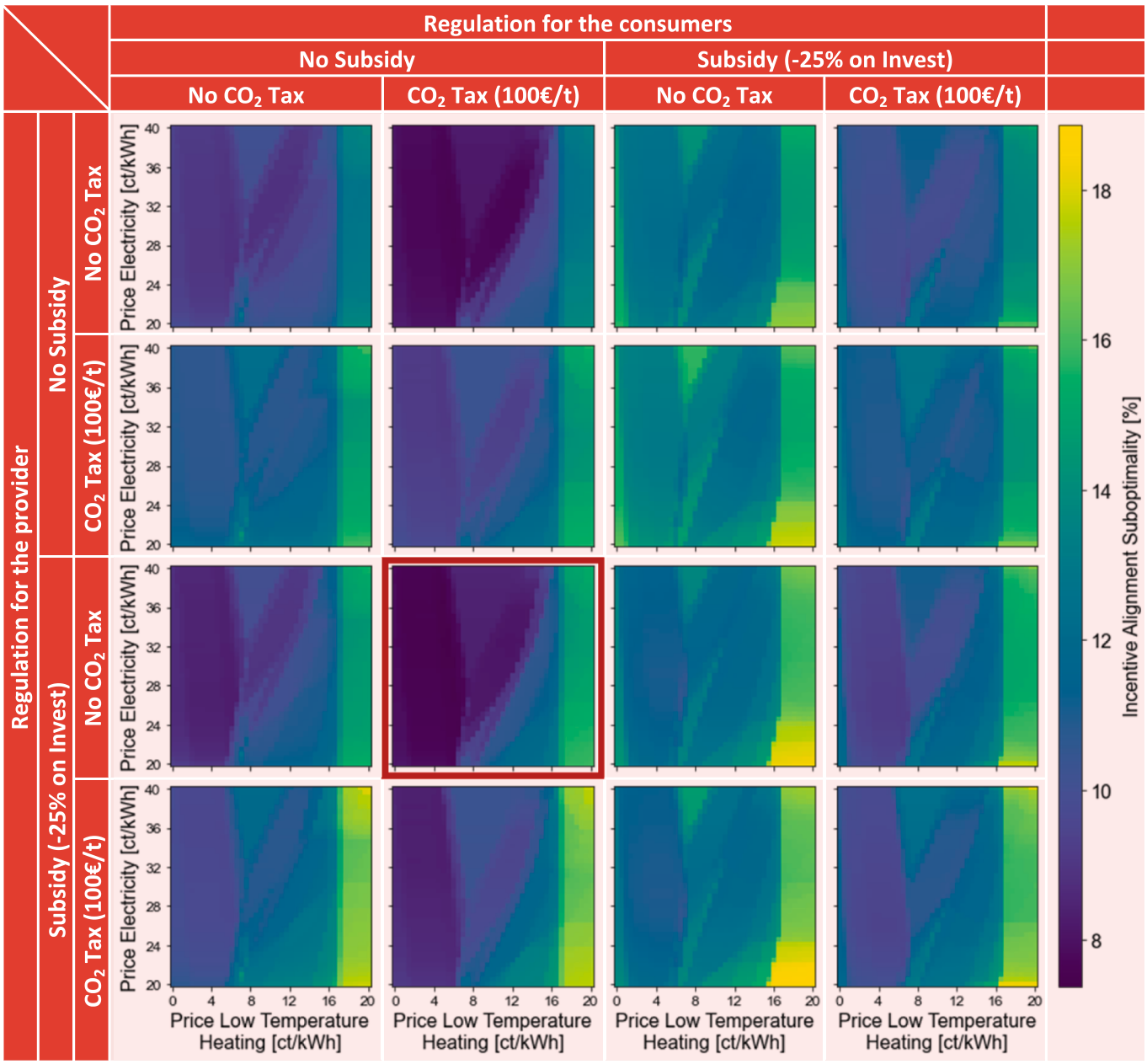

Fig. 11. The incentive alignment suboptimalities depending on CO_2 taxes and subsidies for climate-friendly technologies.

to derive fields for future research.

Answer to the research questions

1 How do multi-agent energy system models differ from traditional central-planner models in terms of cost, self-consumption, and coordination efficiency?

Multi-agent models reveal efficiency losses of 8–18% compared to central planning due to non-aligned incentives and price barriers. Central planning achieves higher self-consumption and cost efficiency by coordinating investment and operation across agents. Traditional models that neglect stakeholder behavior may underestimate system costs and overstate emission savings.

2 What impact do fixed-price contracts have on consumer investment behavior, system costs, and CO_2 emissions? Can regulatory instruments like price ceilings improve outcomes?

Fixed-price contracts, especially those exceeding 16.5 ct/kWh for low-temperature heat, cause consumers to shift to CO_2-intensive high-temperature sources. Such misalignments emerge from the gap between system-optimal marginal costs and contractually agreed tariffs. Introducing price ceilings or time-variable tariffs can counteract these distortions, aligning individual decisions with socially beneficial outcomes. This also supports emerging German legislation promoting time-variable and marginal cost-reflective pricing [123].

3 How can regulation align incentives between decentralized actors? Which combinations of taxes and subsidies are most effective in reducing welfare losses and emissions?

4 Regulatory measures such as CO_2 taxes and investment subsidies not only shift optimal system configurations (primary effect) but also influence the degree of incentive alignment between agents (secondary effect). In this study, a regulation scheme combining a 100 €/t CO_2 tax for consumers with a 25% investment subsidy for the provider reduced the incentive misalignment from 8.8% to 7.3%, while also cutting emissions and preserving cost neutrality for the regulator. These findings suggest that balanced schemes combining sticks and carrots outperform single-measure policies.

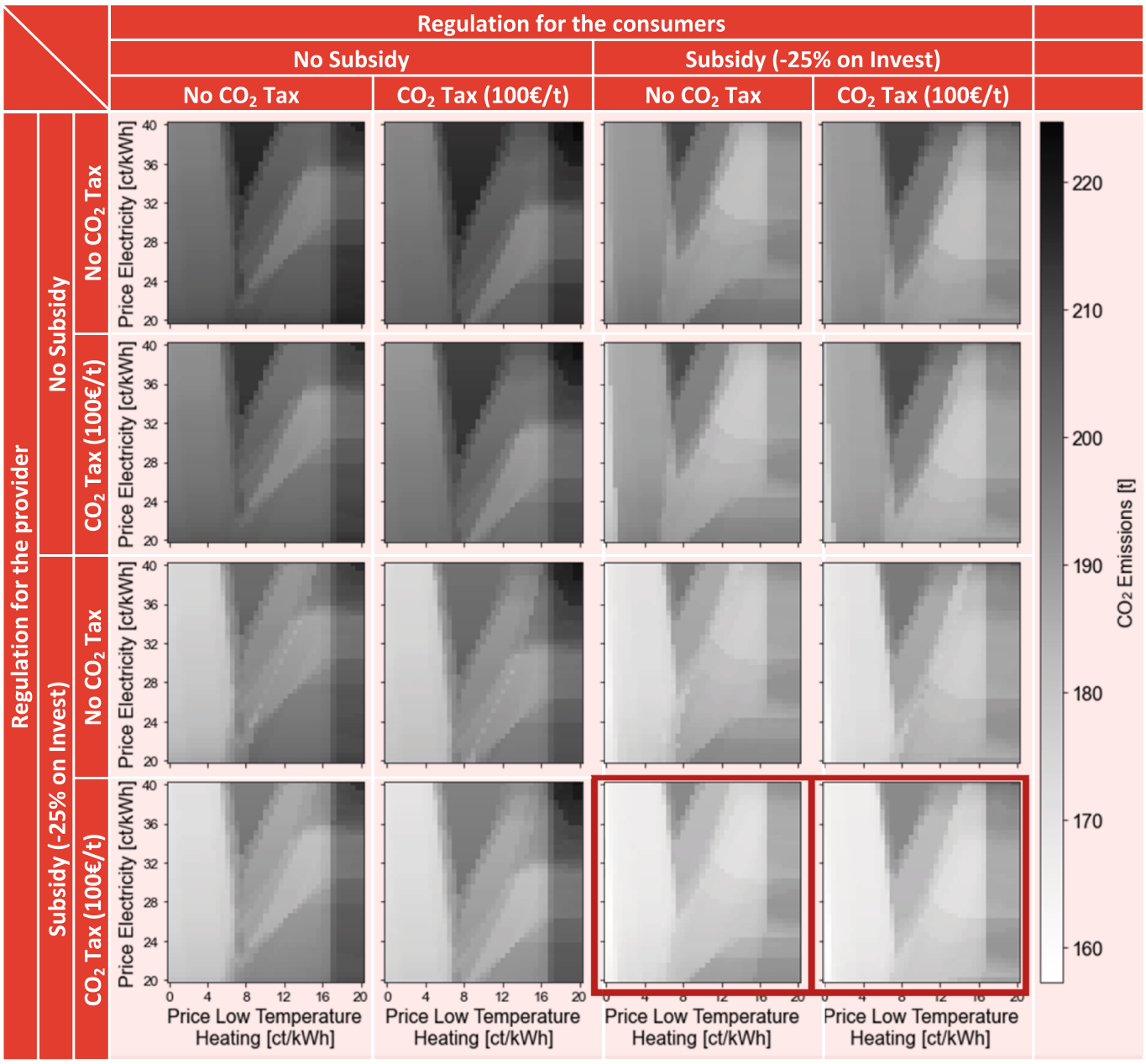

Fig. 12. CO_2 emissions depending on CO_2 taxes and subsidies for climate-friendly technologies.

Political implications

This study highlights a fundamental challenge in decentralized energy systems: the misalignment of incentives between energy consumers and providers under fixed-price contracts. Constant price structures, though simple to implement, fail to reflect marginal costs and system-wide efficiency, leading to distorted investment signals.

The findings resonate with ongoing regulatory debates across Europe. For example, Art. 24(4b) of the EU directive RED III [124] mandates third-party access to district heating networks for renewable heat providers. While beneficial for decarbonization, this can create conflicts if pricing and infrastructure access are not aligned.

Similarly, Germany's Energy Industry Act (§14a, §41a EnWG) [123] introduces dynamic tariffs and grid-optimized appliance control, but German models for "citizen energy companies" (Bürgerenergiegesellschaften) lack provisions for grid-based energy sharing [125,126], an essential condition for energy communities as envisioned in the EU directives RED II Art. 22 and IMED Art. 16 [94,127].

Countries like Switzerland have taken more proactive steps: legal frameworks such as ZEV (Zusammenschluss zum Eigenverbrauch, Art. 17 & 18, EnG) [128] and LEG (Lokale Elektrizitätsgemeinschaft, Art. 17d, StromVG) [129] already enable shared infrastructure and coordinated dispatch.

Our model results, together with these examples, suggest that legislation could facilitate coordinated price signals, infrastructure sharing, and fair access, supported by digital infrastructure such as smart meters, which is consistent with previous work highlighting the importance of aligning economic incentives with system-level efficiency in energy systems [130]. In this context, regulatory schemes combining CO_2 taxes with investment subsidies emerge as potentially effective instruments to both shift behavior and balance public budgets. However, these policy implications should be interpreted as indicative rather than prescriptive, as they are derived from a stylized modeling framework that does not fully capture real-world institutional, behavioral, and

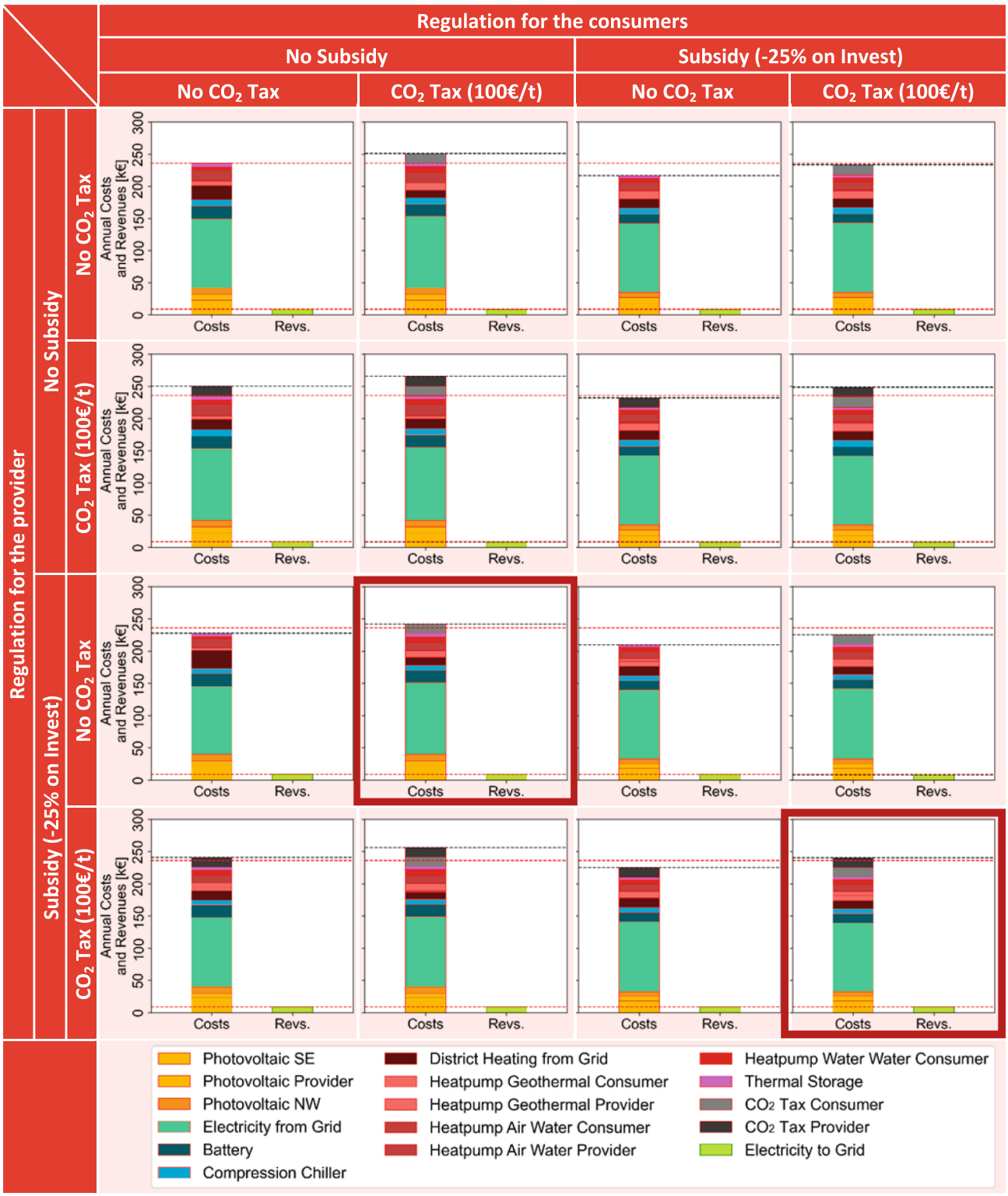

Fig. 13. Annualized costs and revenues of the macro model depending on CO_2 taxes and subsidies for climate-friendly technologies.

market complexities.

Methodological limitations and future work

The discretized Stackelberg model applied here offers a computationally tractable alternative to traditional bilevel formulations. By presolving consumer responses to discrete price vectors, this study sidesteps the complexity of KKT-based transformations often found in MPECs [78,80,81]. This makes the model scalable to full district representations with dozens of agents. However, this approach also imposes limitations. The discretization restricts price-setting to a predefined grid, possibly missing locally optimal configurations as well as a potential global optimum outside of the investigated price combinations. Additionally, the discretization effort increases exponentially with the number of price vectors considered. In this study, the analysis was restricted to two price vectors—electricity and low-temperature heat—each varied over a 20

ct/kWh range with a step size of 0.5 ct/kWh, resulting in $41^2 = 1{,}681$ separate optimizations per building and regulatory setting. Extending the approach to a third price vector with the same range and resolution would increase the computational demand to $41^3 = 68{,}921$ optimizations. Consequently, the proposed methodology is feasible only for a limited number of commodity prices.

The proposed method of separating the stakeholders' subsystems also relies on a number of simplifying technical assumptions such as not modeling infrastructure costs, explicit temperature levels, or heat losses in the high- and low-temperature networks. While these simplifications improve computational tractability and allow separation into consumer- and provider-side subsystems, they may limit the model's ability to fully capture interactions between network design, consumer behavior, and system efficiency. In particular, fixed temperature levels and separate low-temperature and cooling loops were assumed, which precludes adaptive control of network temperatures and mass flows as implemented in real bidirectional 5GDHC systems and may bias efficiency-related results. While temperature-dependent coefficients of performance (COPs) are accounted for at the component level as described in Appendix A.4, the absence of a fully coupled thermo-hydraulic network model limits the comparability of the presented results with state-of-the-art, physics-driven district heating and cooling simulations.

Apart from that, the model assumes single-period, overnight investments and therefore simplifies investment timing which is crucial for modeling system evolution of national [131] but also 5GDHC systems [64] over time and accounting for technological progress [18]. Behavioral drivers, such as environmental preferences or co-investment with electric vehicles, are not yet represented in the model but may be crucial to reflect consumer decision-making in real life.

Furthermore, the model uses a single weather year and hourly resolution. While this keeps run times manageable, the simulation of higher temporal granularity is often necessary for components like inverters or storage systems [132–135].

Moreover, emerging technologies such as bidirectional EV charging or seasonal storage, and new energy sources such as data center waste heat were beyond the current model scope but could be considered in future work.

Conclusion

This study highlights the critical role of pricing strategies and regulatory design in aligning stakeholder incentives and optimizing the performance of decentralized fifth-generation district heating and cooling (5GDHC) systems. By using a discretized Stackelberg pricing game to model the interactions between one price-setting energy provider and 51 price-taking consumers in a real-world residential district currently built and operated in Hassel, Germany, as part of the TransUrban.NRW project, this study quantifies both economic inefficiencies and emission outcomes under various contractual and regulatory constellations.

The results reveal that investment decisions of consumers become increasingly complex as electricity becomes cheaper and heating more expensive, often leading to the deployment of multiple heat pumps operating at different temperature levels. This behavior is highly sensitive to price signals and illustrates the dependency of efficient system layouts on future price trends.

Importantly, pricing low-temperature heat above 16.5 ct/kWh leads to a substantial shift toward high-temperature district heating (HTH), which is both costlier and more carbon-intensive. This shift contributes to a misalignment with the social welfare optimum and suggests that price ceilings could help to prevent economically and ecologically suboptimal outcomes. Conversely, pricing low-temperature heat around 6 ct/kWh minimizes the deviation from the social welfare optimum but is not the profit-optimal choice for the energy provider, highlighting a central regulatory dilemma: achieving macroeconomic efficiency while maintaining provider viability.

This work introduces and applies the incentive alignment suboptimality metric to quantify the economic inefficiencies resulting from fixed-price interactions. Even in best-case scenarios, static contracts without additional regulation lead to welfare losses of at least 8.8%, which rise to 14% if low-temperature heat is priced above 16.5 ct/kWh. These results provide indicative evidence supporting dynamic pricing schemes, ideally based on marginal costs, as promoted by §41a EnWG in Germany, and in line with EU RED II and IMED directives, as well as Swiss EnG and StromVG frameworks that enable energy communities and dynamic, shared energy use.

Regulation appears to be a key lever for mitigating coordination failures. A CO_2 tax of 100 €/t imposed on consumers combined with a 25% investment subsidy for providers can reduce the system misalignment from 8.8% to 7.3% while maintaining financial neutrality for the regulator. This configuration is associated with low LTH pricing, facilitates provider profitability, and improves coordination across actors. For emission reduction, the most effective scheme involves imposing both CO_2 taxes and investment subsidies on both consumers and providers, balancing financial flows and achieving significant CO_2 mitigation.

In summary, the findings emphasize that dynamic, marginal-cost-reflective pricing, liberalized energy sharing within communities, and "carrot-and-stick" regulation combining subsidies and taxation may contribute to unlocking the full potential of 5GDHC systems. These measures are associated with lower system costs and emissions and may improve the alignment of stakeholder incentives with the social welfare optimum, which is important for achieving a resilient, decarbonized heat sector. However, these findings should be interpreted with caution, as they are derived from a stylized modeling framework. Real-world outcomes may differ due to institutional constraints, behavioral heterogeneity, and market dynamics not fully captured in the model.

Declaration of Generative AI and AI-assisted technologies in the writing process

During the preparation of this work the authors used ChatGPT in order to improve language and readability. After using this tool, the authors reviewed and edited the content as needed and take full responsibility for the content of the publication.

CRediT authorship contribution statement

Maximilian Hoffmann: . **Frieder Borggrefe:** Writing – review & editing, Supervision, Project administration, Conceptualization. **Detlef Stolten:** Supervision. **Aaron Praktiknjo:** Supervision, Project administration, Funding acquisition.

Declaration of competing interest

The authors declare that they have no known competing financial interests or personal relationships that could have appeared to influence the work reported in this paper.

Acknowledgements

We gratefully acknowledge financial support by the Federal Ministry for Economic Affairs and Energy (BMWE), Germany, promotional reference: 03EWR020E (Reallabor der Energiewende: TransUrban.NRW). Furthermore, this work was supported by the Helmholtz Association under the program "Energy System Design".

Appendix

A.1. Table of 5GDHC terminologies

Table 4
Different terms for low-temperature heating and cooling networks used in the literature.

Publication			Term						
	Year	Reference	5th generation heating and cooling	Bidirectional low temperature networks	(Ultra-) low temperature district heating and cooling	Thermal source networks	Anergy grids or anergy networks	Cold district heating networks	Balanced energy heating networks
Chicherin et al.	2025	[51]	✖						
Gjoka	2025	[52]	✖						
Hachez et al.	2025	[53]	✖						
Boussaid et al.	2024	[54]	✖						
Chaudry et al.	2024	[55]	✖						
Halilovic et al.	2024	[56]	✖						
Soleimani et al.	2024	[56]	✖						
Zhang et al.	2024	[57]	✖		✖				
Abugabbara et al.	2023	[58]	✖						
Bu et al.	2023	[59]	✖	✖					
Buonomano et al.	2023	[60]	✖						
Qin et al.	2023	[61]	✖	✖					
Qin et al.	2023	[62]	✖	✖					
Wirtz	2023	[63]	✖						
Wirtz et al.	2023	[64]	✖						
Wirtz et al.	2023	[65]	✖						
Zhang et al.	2023	[66]	✖		✖				
Calise et al.	2022	[67]	✖						
Meibodi and Loveridge	2022	[68]	✖						

(continued on next page)

Table 4 (*continued*)

Publication			Term						
	Year	Reference	5th generation heating and cooling	Bidirectional low temperature networks	(Ultra-) low temperature district heating and cooling	Thermal source networks	Anergy grids or anergy networks	Cold district heating networks	Balanced energy heating networks
Bilardo et al.	2021	[30]	✖						
Edtmayer et al.	2021	[69]	✖						
Hering et al.	2021	[70]	✖						
Lund et al.	2021	[71]	✖						
Reiners et al.	2021	[72]	✖						
Wirtz et al.	2021	[73]	✖						
Abugabbara	2020	[74]	✖						
Buffa et al.	2020	[75]	✖						
Revesz et al.	2020	[76]	✖						
Wirtz et al.	2020	[6]	✖						
Buffa et al.	2019	[23]	✖					✖	
Boesten et al.	2019	[22]	✖						
von Rhein et al.	2019	[77]	✖						
Abugabbara et al.	2024	[27]		✖					
Dibos et al.	2024	[28]		✖	✖				
Zhou et al.	2023	[29]		✖	✖				
Bilardo et al.	2021	[30]		✖					
Wirtz et al.	2020	[21]		✖					
Wirtz et al.	2019	[5]		✖					
Zarin Pass et al.	2018	[31]		✖					
Bünning et al.	2018	[32]		✖					
Quirosa et al.	2023	[46]			✖				
Quirosa et al.	2022	[47]			✖				
Sommer et al.	2020	[48]			✖				
Sommer et al.	2019	[49]			✖				

(*continued on next page*)

Table 4 (*continued*)

Publication			Term						
	Year	Reference	5th generation heating and cooling	Bidirectional low temperature networks	(Ultra-) low temperature district heating and cooling	Thermal source networks	Anergy grids or anergy networks	Cold district heating networks	Balanced energy heating networks
Ruesch and Haller	2017	[50]			✖				
Lagoeiro et al.	2026	[34]				✖			
Etemad et al.	2025	[35]				✖			
Etemad et al.	2025	[36]				✖			
Müller et al.	2025	[37]				✖			
Lund et al.	2024	[39]				✖			
Belfiore et al.	2021	[42]					✖		
Gabrielli et al.	2020	[43]					✖		
Zach et al.	2019	[44]					✖		
Pellegrini and Bianchini	2018	[40]						✖	
Stubler et al.	2014	[41]						✖	
Song et al.	2019	[45]							✖

A.2. Table of costs

Table 5
Cost parameters for the model.

	Capex				Opex		Lifetime		Source
Components	Fixed		Capacity-Specific		Fixed + Capacity-Specific				
PV Rooftop	—	—	769.00	€/kW_p	1.00	% Inv./a	20	a	[136]
Inverter	—	—	75.00	€/kW_p	—	—	20	a	[137]
Battery	—	—	301.00	€/kWh_p	—	—	15	a	[136]
Heat Pump (Air/Water)	4,230.00	€	504.90	€/kW_{th}	1.50	% Inv./a	20	a	[138]
Heat Pump (Geothermal)	2,201.11	€	1,801.27	€/kW_{th}	1.50	% Inv./a	20	a	[138]
Compression Chiller	4,230.00	€	504.90	€/kW_{th}	1.50	% Inv./a	20	a	[138]
Thermal Storage	—	—	90.00	€/kWh_{th}	0.01	% Inv./a	25	a	[139]

A.3. Individual consumer data

Heating and cooling demands were simulated using the open-source tool TEASER [140], while domestic hot water demand profiles were generated using DHWcalc [141]. For all weather-related simulations, the year 2015 from the German Weather Service (DWD) for Gelsenkirchen-Hassel was used [142]. Electricity demand and PV capacity factor profiles were produced with the open-source tool tsib [143], which builds on the probabilistic CREST model [144]. Required input data included building age, area, location, number of apartments, and household size, based on internal project documentation [109]. All time series are modeled with hourly resolution to balance detail and computational tractability [133].

The demand profiles for all buildings are shown in Figure 14. Profiles vary in amplitude depending on building type: single-family homes and terraced houses (locations 0–35) versus apartment buildings (locations 37–51). Environmental factors (e.g., temperature, solar radiation) drive the correlation in heating, cooling, and PV profiles across buildings, whereas electricity and hot water demands are shaped by occupant behavior and therefore less correlated.

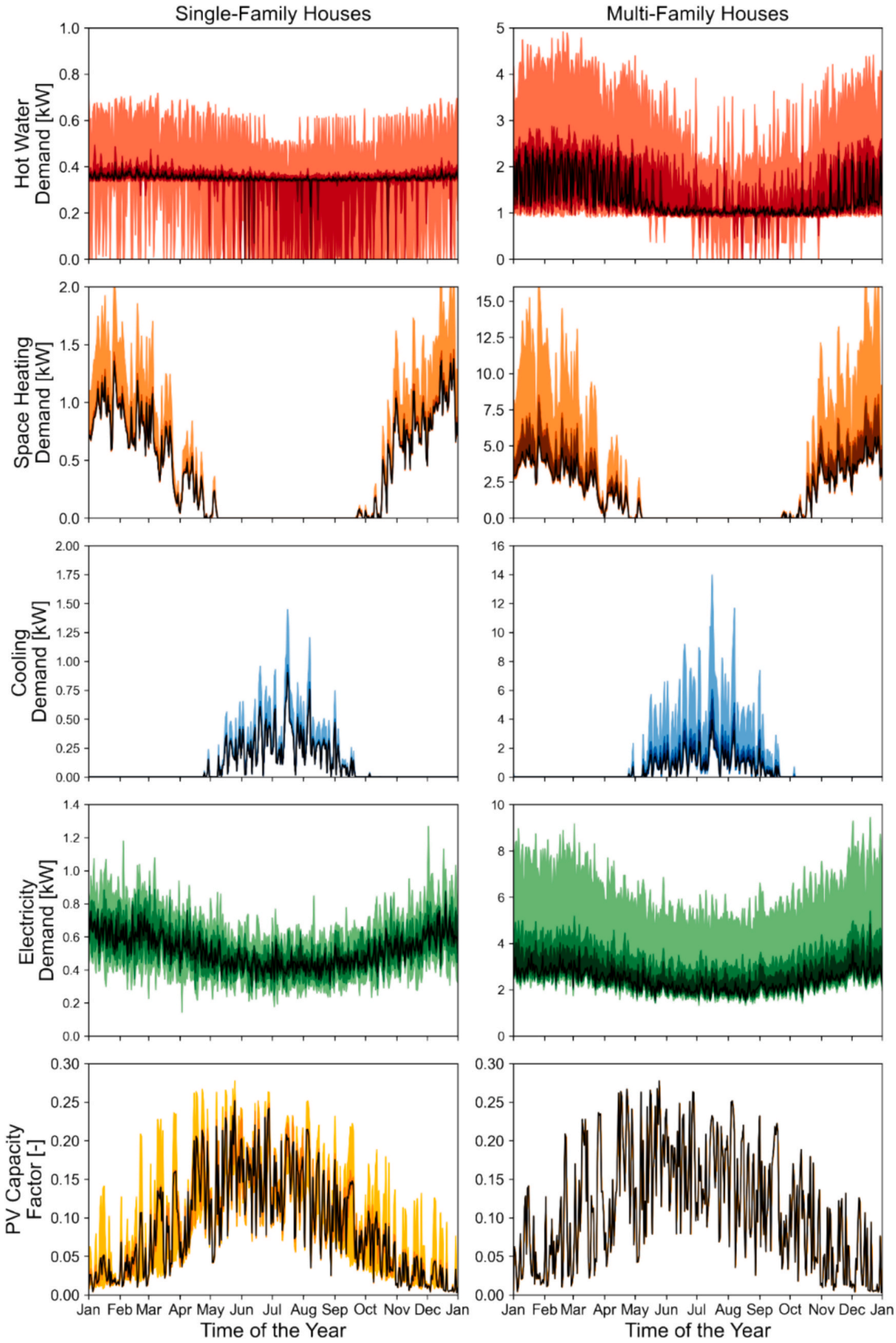

Fig. 14. Daily mean value profiles for the four demand and one capacity factor time series for all single- and multi-family houses.

A.4. Model formulation

The following subsections provides a more detailed formulation of the bottom-up energy system model introduced in Subsection 3.1, its decomposition into the provider and multiple consumers introduced in Subsection 3.2 and the implementation of regulation schemes introduced in Subsection 3.3.

Basic bottom-up energy system model.

First, optimization-based bottom-up energy system models such as ETHOS.FINE [12,114] generally comprise certain components such as commodity sinks, sources, transmission units, storage components, conversion units and energy hubs. Here, commodities may refer to energy carriers such as electricity, heat, natural gas or hydrogen, but also to mass flows such as CO_2. An overview of these components is provided in Figure 15. Here, the model comprises two regions which are connected by a transmission unit for the "blue" commodity, which may, e.g., refer to electricity. The "red" commodity, which may refer to heat, is locally produced and consumed in Region 2 by converting the blue commodity into the red one. Here, the conversion unit may refer to an electric heater or a heat pump.

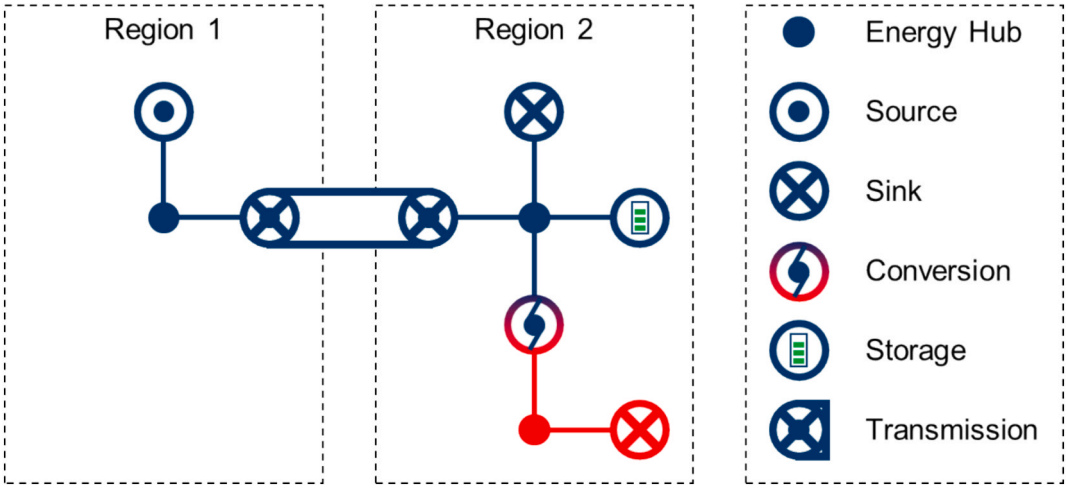

Fig. 15. Basic concept of the system components in energy system frameworks such as ETHOS.FINE [12,114] taken from Hoffmann et al. [145].

The overall optimization problem is formulated in Eqs. (2)–(16) and is a modified version of the model presented by Hoffmann et al. [145]. Similar model descriptions can be found in the literature, e.g., as published by [146] and [12].

Eq. (2) describes the objective function to minimize the total costs of the annualized capacity investment costs $c_{c,r}^{cap} x_{c,r}^{cap}$, annualized binary investment costs $c_{c,r}^{cap,bin} x_{c,r}^{cap,bin}$ (if a component is built or not) and the operation costs $c_{c,r,t}^{op} x_{c,r,t}^{op}$ for all components c, regions r and time steps t. Eqs. (3)–(7) must hold for every commodity $g \in G$, region $r \in R$ and time step $t \in T$. Eq. (3) maintains the flow conservation at each energy hub for each commodity, region and time step, i.e. the sum of flows from all components emitting this commodity must equal the sum of flows to all components consuming it, which is represented by $c \in M^g$. Eqs. (4) and (5) state that the energy flows are positive for energy sources and negative for energy sinks. Eq. (6) states that for conversion units, the flow of a commodity depends on a conversion factor γ. These may be positive or negative for different commodities associated with the same conversion unit, e.g. a heat pump would consume electricity (negative conversion factor) for producing heat (positive conversion factor). Eq. (7) states that the net flow for transmission units starting in a Region r and ending in another Region r′ equals the flow from r′ to r minus the flow from r to r′.

Eqs. (8)–(16) are defined for each region $r \in R$ and time step $t \in T$. Here, Eq. (8) states that each operation rate $x_{c,r,t}^{op}$ must be positive. Further, Eq. (9) states that it must not be larger than the capacity of the installed unit times the operation rate θ times the duration of the respective discrete time step Δt, e.g. a PV system with 5 kW installed capacity and a capacity factor of 0.5 in an hourly time step may not produce more than 2.5 kWh of electricity in the respective time step. Eqs. (10)–(12) address storage units. Eq. (10) states that the state of charge of a storage in the next time period equals the current state of charge plus inflows times the charging efficiency minus outflows divided by the discharge efficiency. Here, a self-discharge rate for the state of charge may also be set in front of the state of charge of the current period. Eqs. (11) and (12) state that the state of charge of storage components must be positive and smaller than the respective capacity. Eqs. (13)–(16) address the transmission units. Here, Eq. (13) states that the operation in either direction must be non-negative. Eqs. (14) and (15) state that the net flows in either direction are capped by the capacity of the transmission line times the time step length Δt. Eq. (16) states that the sum of flows should also be smaller than the installed capacity. This equation must not be interpreted physically, but is just a cut in the optimization model which avoids infinitely high operation rates in either direction with a finite net flow, i.e. it only contributes to the numeric stability of the energy system model. Eq. (17) states that energy components may not surpass a certain capacity given by the respective potential. This constraint may be defined for all components, but does not need to, and refers to e.g. limited roof area for PV panels. Lastly, the Eqs. (18) and (19) make up the set of BigM constraints and the corresponding variable domain constraints defining that if a component's capacity is larger than zero, it is built and accordingly, the binary investment costs are added to the objective function. These variables allow for an affine modeling of cost curves and thereby economies of scale in a simplified manner, but turn the LP into an MILP. For that reason, they may also be ignored if the cost curves are approximately linear.

$$\min\left(\sum_c\sum_r\left(c_{c,r}^{cap}x_{c,r}^{cap}+c_{c,r}^{cap,bin}x_{c,r}^{cap,bin}+\sum_t c_{c,r,t}^{op}x_{c,r,t}^{op}\right)\right) \tag{2}$$

s.t.

$\forall g \in G,\ r \in R,\ t \in T:$

$$\sum_{c\in M^g} f_{c,g,r,t} = 0 \tag{3}$$

$$f_{c,g,r,t} = x_{c,r,t}^{op} \forall\ c \in M^{source} \cap M^g \tag{4}$$

$$f_{c,g,r,t} = -x_{c,r,t}^{op} \forall\ c \in M^{sink} \cap M^g \tag{5}$$

$$f_{c,g,r,t} = \gamma_{c,g,r,t}x_{c,r,t}^{op} \forall\ c \in M^{conversion} \cap M^g \tag{6}$$

$$f_{c,g,r,t} = x_{c,(r',r),t}^{op} - x_{c,(r,r'),t}^{op} \forall\ c \in M^{transmission} \cap M^g \tag{7}$$

$\forall r \in R,\ t \in T:$

$$x_{c,r,t}^{op} \geq 0 \forall\ c \in M^{source} \cup M^{sink} \cup M^{conversion} \tag{8}$$

$$x_{c,r,t}^{op} \leq \theta_{c,r,t}x_{c,r}^{cap}\Delta t \forall\ c \in M^{source} \cup M^{sink} \cup M^{conversion} \tag{9}$$

$$x_{c,r,t+1}^{SOC} = \left(1-\eta_{c,r,t}^{op,sd}\right)x_{c,r,t}^{SOC} + \eta_{c,r,t}^{ch}x_{c,r,t}^{op,ch} - \frac{x_{c,r,t}^{op,dis}}{\eta_{c,r,t}^{dis}} \forall\ c \in M^{store} \tag{10}$$

$$x_{c,r,t}^{SOC} \geq 0 \forall\ c \in M^{store} \tag{11}$$

$$x_{c,r,t}^{SOC} \leq x_{c,r}^{cap} \forall\ c \in M^{store} \tag{12}$$

$$x_{c,(r,r'),t}^{op} \geq 0 \forall\ c \in M^{transmission}, r' \in R\backslash\{r\} \tag{13}$$

$$-x_{c,r}^{cap}\Delta t \leq x_{c,(r',r),t}^{op} - x_{c,(r,r'),t}^{op} \forall\ c \in M^{transmission}, r' \in R\backslash\{r\} \tag{14}$$

$$x_{c,r}^{cap}\Delta t \geq x_{c,(r',r),t}^{op} - x_{c,(r,r'),t}^{op} \forall\ c \in M^{transmission}, r' \in R\backslash\{r\} \tag{15}$$

$$x_{c,r}^{cap}\Delta t \geq x_{c,(r',r),t}^{op} + x_{c,(r,r'),t}^{op} \forall\ c \in M^{transmission}, r' \in R\backslash\{r\} \tag{16}$$

$$x_{c,r}^{cap} \leq \overline{x}_{c,r}^{pot} \forall\ c \in M^{source} \cup M^{sink} \cup M^{conv} \cup M^{trans} \tag{17}$$

$$x_{c,r}^{cap} \leq Mx_{c,r}^{cap,bin} \forall\ c \in M^{source} \cup M^{sink} \cup M^{conv} \cup M^{trans} \tag{18}$$

$$x_{c,r}^{cap,bin} \in \{0,1\} \forall\ c \in M^{source} \cup M^{sink} \cup M^{conv} \cup M^{trans} \tag{19}$$

Model decomposition into multiple stakeholders

The central-planner model as stated above can be divided into the subsystems of the energy providers and the consumers so that each component (irrespectively whether these are sources, sinks, conversion units or transmission lines) of the original model is assigned to exactly one of the stakeholders, i.e. the following must hold:

$$M_{provider}^{type} \underset{i\in\{1,\cdots 51\}}{\cup} M_{consumer,i}^{type} = M^{type} \tag{20}$$

$$M_{provider}^{type} \cap M_{consumer,i}^{type} = \varnothing \forall i \in \{1,\cdots 51\} \tag{21}$$

$$M_{consumer,i}^{type} \cap M_{consumer,j}^{type} = \varnothing \forall i,j \in \{1,\cdots 51\},\ i \neq j \tag{22}$$

$$\text{with type} \in \{\text{source, sink, conversion, transmission}\} \tag{23}$$

As the energy consumers are now separated from the energy provider, the commodity flows from the energy provider to the consumers or vice versa have to be respected by means of auxiliary source- and sink pairs, i.e. every flow from the provider to a consumer becomes a source in the consumer

model and a sink in the provider model. In case of a reversed flow (e.g., electricity feed-in from the consumer) an auxiliary sink is needed in the consumer model and a source in the provider model. For that reason, Eq. (3) is adapted as follows in all the consumer models:

$$\sum_{c \in M^{g}_{consumer,i}} f_{c,g,r,t} + f_{BoughtByConsumer,g,r,t} + f_{SoldByConsumer,g,r,t} = 0 \; \forall g \in G,\, r \in R,\, t \in T \tag{24}$$

Here, the commodity flow bought by the consumer is defined to be positive, whereas the one sold by the consumer is defined negative. For the operation rates of the corresponding source and sink, which are defined as positive thus holds:

$$f_{BoughtByConsumer,g,r,t} = x^{op}_{auxConSource,g,r,t} \tag{25}$$

$$f_{SoldByConsumer,g,r,t} = -x^{op}_{auxConSink,g,r,t} \tag{26}$$

The respective objective function is complemented by the expenditures for buying the commodities from the provider and by the revenues from feeding in commodities to the provider, i.e.:

$$\min\left(\sum_{c \in M_{consumer,i}} \sum_{r} \left(c^{cap}_{c,r} x^{cap}_{c,r} + c^{cap,bin}_{c,r} x^{cap,bin}_{c,r} + \sum_{t} c^{op}_{c,r,t} x^{op}_{c,r,t}\right) + \sum_{g} \sum_{r} \sum_{t} p_{g} x^{op}_{auxConSource,g,r,t} - \overline{p}_{g} x^{op}_{auxConSink,g,r,t}\right) \tag{27}$$

Here, p_g denotes the price for which the commodity g is offered by the provider and $\overline{p}_g$ is the price for which the commodity g can be fed in to the provider. The equations for the energy provider are analogous, i.e.:

$$\sum_{c \in M^{g}_{consumer,i}} f_{c,g,r,t} + f_{BoughtByProvider,g,r,t} + f_{SoldByProvider,g,r,t} = 0 \; \forall g \in G,\, r \in R,\, t \in T \tag{28}$$

$$f_{BoughtByProvider,g,r,t} = x^{op}_{auxProvSource,g,r,t} \tag{29}$$

$$f_{SoldByProv,g,r,t} = -x^{op}_{auxProvSink,g,r,t} \tag{30}$$

$$\min\left(\sum_{c \in M_{provider}} \sum_{r} \left(c^{cap}_{c,r} x^{cap}_{c,r} + c^{cap,bin}_{c,r} x^{cap,bin}_{c,r} + \sum_{t} c^{op}_{c,r,t} x^{op}_{c,r,t}\right) + \sum_{g} \sum_{r} \sum_{t} p_{g} x^{op}_{auxProvSource,g,r,t} - \overline{p}_{g} x^{op}_{auxProvSink,g,r,t}\right) \tag{31}$$

The prices p_g and $\overline{p}_g$ trigger the behavior of the consumers and thereby the operation of the auxiliary sources and sinks, i.e. what they buy from the provider and when. As the energy provider has to provider what is sold by the consumers, and has to buy what is fed in by the consumers, the following holds:

$$x^{op}_{auxProvSource,g,r,t} = \sum_{i \in \{1,\cdots,51\}} x^{op,consumer,i}_{auxConSink,g,r,t} \tag{32}$$

$$x^{op}_{auxProvSink,g,r,t} = \sum_{i \in \{1,\cdots,51\}} x^{op,consumer,i}_{auxConSource,g,r,t} \tag{33}$$

Plugging these relationships into the objective function of the provider yields:

$$\min\left(\sum_{c \in M_{provider}} \sum_{r} \left(c^{cap}_{c,r} x^{cap}_{c,r} + c^{cap,bin}_{c,r} x^{cap,bin}_{c,r} + \sum_{t} c^{op}_{c,r,t} x^{op}_{c,r,t}\right) + \sum_{g} \sum_{r} \sum_{t} p_{g} \sum_{i \in \{1,\cdots,51\}} x^{op,consumer,i}_{auxConSink,g,r,t} - \overline{p}_{g} \sum_{i \in \{1,\cdots,51\}} x^{op,consumer,i}_{auxConSource,g,r,t}\right) \tag{34}$$

And summing over all consumers yields for the cumulative consumer objective:

$$\min\left(\sum_{i \in \{1,\cdots,51\}} \sum_{c \in M_{consumer,i}} \sum_{r} \left(c^{cap}_{c,r} x^{cap}_{c,r} + c^{cap,bin}_{c,r} x^{cap,bin}_{c,r} + \sum_{t} c^{op}_{c,r,t} x^{op}_{c,r,t}\right) + \sum_{g} \sum_{r} \sum_{t} p_{g} \sum_{i \in \{1,\cdots,51\}} x^{op,consumer,i}_{auxConSource,g,r,t} - \overline{p}_{g} \sum_{i \in \{1,\cdots,51\}} x^{op,consumer,i}_{auxConSink,g,r,t}\right) \tag{35}$$

Adding up the objective functions in Eqs. (41) and (42) yields given the telescopic sum of auxiliary sinks and sources:

$$\begin{aligned} &\min\left(\sum_{c \in M_{provider}} \sum_{r} \left(c^{cap}_{c,r} x^{cap}_{c,r} + c^{cap,bin}_{c,r} x^{cap,bin}_{c,r} + \sum_{t} c^{op}_{c,r,t} x^{op}_{c,r,t}\right) + \sum_{i \in \{1,\cdots,51\}} \sum_{c \in M_{consumer,i}} \sum_{r} \left(c^{cap}_{c,r} x^{cap}_{c,r} + c^{cap,bin}_{c,r} x^{cap,bin}_{c,r} + \sum_{t} c^{op}_{c,r,t} x^{op}_{c,r,t}\right)\right) \\ &= \min\left(\sum_{c} \sum_{r} \left(c^{cap}_{c,r} x^{cap}_{c,r} + c^{cap,bin}_{c,r} x^{cap,bin}_{c,r} + \sum_{t} c^{op}_{c,r,t} x^{op}_{c,r,t}\right)\right) \end{aligned} \tag{36}$$

because of Eq. (20). Accordingly, the sum of objective functions over all the consumers and the energy provider in the decomposed model equals the objective function of the central planning model. Therefore, all additional costs in the decomposed models arise from non-aligned incentives. Finally,

it must be mentioned that the terms used in this extended analysis refer to the simplified ones in Fig. 3, i.e. the simplified model discussed in Subsection 3.2 is indeed a simplified version notation of the model discussed in this section.

$$F(p,x) \hat{=} \sum_{c \in M_{provider}} \sum_{r} \left(c_{c,r}^{cap} x_{c,r}^{cap} + c_{c,r}^{cap,bin} x_{c,r}^{cap,bin} + \sum_{t} c_{c,r,t}^{op} x_{c,r,t}^{op} \right) + \sum_{g} \sum_{r} \sum_{t} p_g \sum_{i \in \{1,\cdots,51\}} x_{auxConSink,g,r,t}^{op,consumer,i} - \overline{p}_g \sum_{i \in \{1,\cdots,51\}} x_{auxConSource,g,r,t}^{op,consumer,i} \quad (37)$$

$$f(p,x) \hat{=} \sum_{i \in \{1,\cdots,51\}} \sum_{c \in M_{consumer,i}} \sum_{r} \left(c_{c,r}^{cap} x_{c,r}^{cap} + c_{c,r}^{cap,bin} x_{c,r}^{cap,bin} + \sum_{t} c_{c,r,t}^{op} x_{c,r,t}^{op} \right) + \sum_{g} \sum_{r} \sum_{t} p_g \sum_{i \in \{1,\cdots,51\}} x_{auxConSource,g,r,t}^{op,consumer,i} - \overline{p}_g \sum_{i \in \{1,\cdots,51\}} x_{auxConSink,g,r,t}^{op,consumer,i} \quad (38)$$

Implementation of temperature-variable COPs

When modelling the local heating and cooling systems in the different buildings, the efficiency depends on the temperature of the 5GDHC grid. Concisely, the coefficient of performance (COP) of the heat pumps and the compression chiller depend on the temperature differences between the cold and the warm side and were therefore modelled depending on the temperature levels of the heating or cooling networks and the ambient or ground temperature multiplied by a grading factor as percentage of the respective Carnot efficiency, i.e. with T_C being the temperature of the cool and T_H being temperature of the hot side of the Rankine cycle in Kelvin (c.f. [8]):

$$COP_{\text{Heat Pump}} = \eta_{grade} \frac{T_H}{T_H - T_C} \quad (39)$$

$$COP_{\text{Compression Chiller}} = \eta_{grade} \frac{T_C}{T_H - T_C} \quad (40)$$

Here, the grading factors for the air–water and water-water heat pumps as well as the compression chiller were assumed to be 40%, whereas they were assumed to be 55% for the geothermal heat pumps in accordance with the assumptions in the documentation of the oemof modelling framework [147,148]. The COPs were capped at a value of 7 in case of too small temperature differences in order to properly capture pressure-loss induced efficiency losses even at small temperature differences [6].

Figure 16 depicts the resulting graphs of the daily averaged COPs for all heat pumps and the compression chiller of the model. Here, it can be seen that the COPs of the water-water heat pump and the compression chiller are constant due to the assumption of constant, i.e. time-independent temperature differences between the district heating, the low-temperature and the cooling networks as well as the ground temperature, whereas the COP of the air–water heat pump and the compression chiller vary throughout the year due to the varying ambient air temperature. Apart from that, it can be seen that the system COP of the air–water heat pump is worst during its main utilization time in winter, whereas the opposite holds for the compression chiller with its main utilization period and respective COP minimum during summer.

In order to improve the coefficient of performance of both, the air–water heat pump and the compression chiller, the temperature levels in the low-temperature and cooling network could be adapted to the ambient temperature and the mass flow could be adapted accordingly. In fact, this adaption takes place in the actual bidirectional network in Hassel in order to lower the provider's electricity demand for operating these units, but cannot be modelled in the current version of ETHOS.FINE appropriately due to the bilinear relationship between energy flow, mass flow and temperature difference between the hot and the cold side.

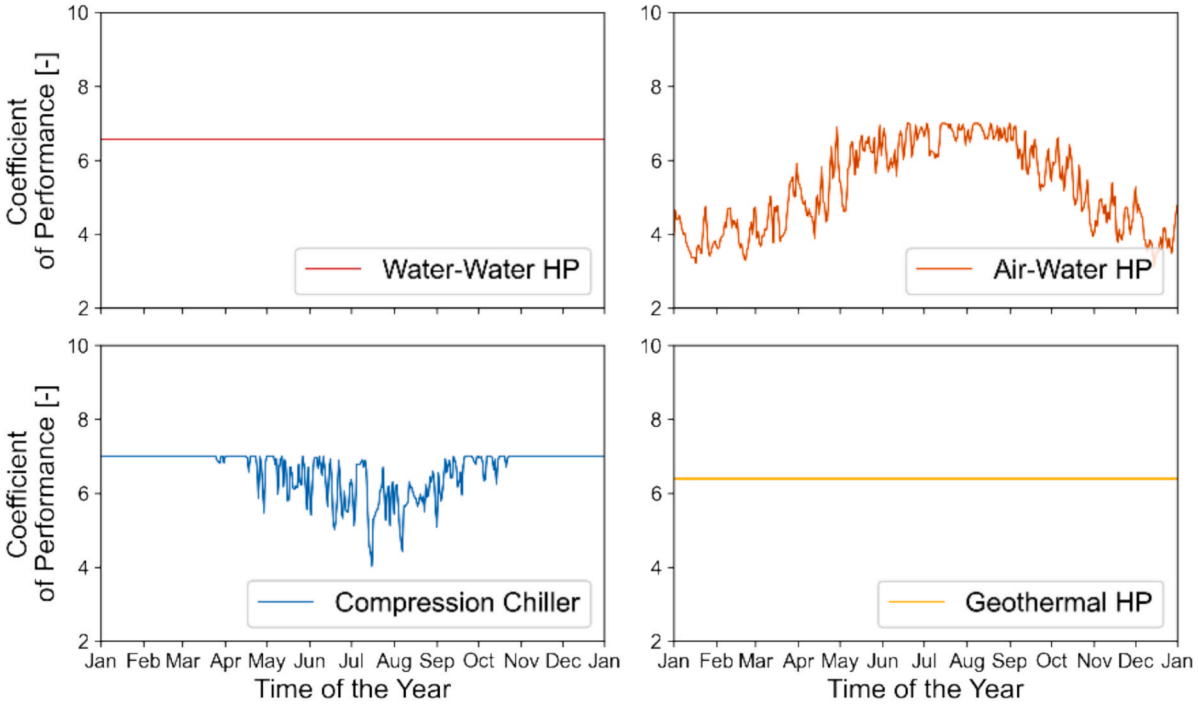

Fig. 16. Yearly coefficients of perffx3ormance for the heat pumps and the compression chiller.

Implementation of regulation measures

The regulations, in particular, subsidies and CO_2 taxes, can be added to the system stated above. For investment subsidies that only affect the cost vector for capacity investments, i.e. the first part of Eq. (2), a discount rate $d_{c,r} \in [0,1]$ may be added as follows:

$$\min\left(\sum_c\sum_r\left((1-d_{c,r})\left(c_{c,r}^{cap}x_{c,r}^{cap}+c_{c,r}^{cap,bin}x_{c,r}^{cap,bin}\right)+\sum_t c_{c,r,t}^{op}x_{c,r,t}^{op}\right)\right) \tag{41}$$

This discount rate is defined for each component and refers to a price release for investment costs, i.e. a discount rate of $d_{c,r}=0.25$ would refer to a discount of 25% for component c in Region r. In contrast to that, the modelling of CO_2 taxes is more complicated. For that, an energy source is transformed into a conversion unit emitting both, energy and CO_2, i.e., Eq. (4) is replaced by two conversion equations as the one in Eq. (6), i.e.:

$$f_{c,g,r,t}=\gamma_{c,g,r,t}x_{c,r,t}^{op},\ \forall r\in R,t\in T \tag{42}$$

$$f_{c,CO_2,r,t}=\gamma_{c,CO_2,r,t}x_{c,r,t}^{op}\forall r\in R,t\in T \tag{43}$$

Additionally, for the original commodity g holds:

$$\gamma_{c,g,r,t}=1\,\forall r\in R,t\in T \tag{44}$$

The conversion factor for CO_2, however, may depend on the specific energy carrier that is provided, e.g. coal has a higher CO_2 emission factor in kg/kWh than natural gas. In order to preserve feasibility, the CO_2 flow balance must be maintained with additional CO_2 hubs and CO_2 sinks:

$$\sum_{c\in\{CO_2\}}f_{c,CO_2,r,t}=0r\in R,\ t\in T \tag{45}$$

$$f_{c,CO_2,r,t}=\gamma_{c,CO_2,r,t}x_{c,r,t}^{op}\forall\ \ r\in R,\ t\in T,c\in M^{conversion}\cap\{CO_2\} \tag{46}$$

$$f_{CO_2-Sink,CO_2,r,t}=-x_{CO_2,r,t}^{op}\forall\ \ r\in R,\ t\in T \tag{47}$$

Here, Eq. (45) refers to the CO_2 flow balance, Eq. (46) states that positive CO_2 flows stem from the system components delivering energy carriers with CO_2 emissions and Eq. (47) states that the CO_2 has to disappear in a CO_2 sink in order to maintain the flow balance. This CO_2 sink does not have to contain a capacity, but may only have an operation rate. Finally, the CO_2 tax may be added to the objective function by multiplying it with the CO_2 costs and summing these emission costs over all regions and time steps as stated in Eq. (48):

$$\min\left(\sum_c\sum_r\left(c_{c,r}^{cap}x_{c,r}^{cap}+c_{c,r}^{cap,bin}x_{c,r}^{cap,bin}+\sum_t c_{c,r,t}^{op}x_{c,r,t}^{op}\right)\right)+\sum_r\sum_t c_{CO_2,r,t}^{op}x_{CO_2,r,t}^{op} \tag{48}$$

As shown, subsidies and CO_2 taxes analyzed in Subsection 4.2, can be directly integrated into an existing energy system model. The consideration of schemes in the regulation decomposed stakeholder models is analogous.

A.5. Total annualized costs per consumer

Table 6 reports the cost-optimal consumer expenditures for cooling, low-temperature heat, district heat and electricity as well as the annualized costs for own system components for a price constellation of 30 ct/kWh for electricity and 10 ct/kWh for low-temperature heat corresponding to Fig. 7.

Table 6
Consumer results for 30 ct/kWh for electricity and 10 ct/kWh for low-temperature heat.

	Cooling		Low-temperature heat		District heating		Electricity from provider		Electricity to provider		Heat pump air water		Heat pump geothermal		Heat pump water water		Thermal storage		Photovoltaic southeast		Photovoltaic northwest		Battery		Sum	
	Abs.	%	Abs.	%	Abs.	%	Abs.	%	Abs.	%	Abs.	%	Abs.	%	Abs.	%	Abs.	%	Abs.	%	Abs.	%	Abs.	%	Abs.	%
loc_0	126	3%	741	20%	874	23%	1164	31%	−334	−9%	0	0%	0	0%	0	0%	105	3%	421	11%	421	11%	261	7%	3779	100%
loc_1	70	4%	400	23%	404	23%	488	28%	−133	−8%	0	0%	0	0%	0	0%	48	3%	210	12%	142	8%	133	8%	1761	100%
loc_2	70	4%	400	23%	402	23%	513	29%	−128	−7%	0	0%	0	0%	0	0%	48	3%	210	12%	124	7%	137	8%	1776	100%
loc_3	126	3%	741	19%	874	23%	1167	31%	−335	−9%	0	0%	0	0%	0	0%	125	3%	421	11%	421	11%	260	7%	3800	100%
loc_4	58	4%	328	21%	352	23%	481	31%	−163	−10%	0	0%	0	0%	0	0%	48	3%	316	20%	0	0%	133	9%	1554	100%
loc_5	58	4%	328	21%	356	23%	456	30%	−157	−10%	0	0%	0	0%	0	0%	45	3%	316	20%	0	0%	139	9%	1541	100%
loc_6	58	4%	328	21%	352	23%	455	29%	−156	−10%	0	0%	0	0%	0	0%	45	3%	316	20%	0	0%	149	10%	1545	100%
loc_7	58	4%	328	20%	354	22%	482	30%	−188	−12%	0	0%	0	0%	0	0%	48	3%	210	13%	210	13%	124	8%	1626	100%
loc_8	58	4%	328	20%	351	21%	488	30%	−190	−12%	0	0%	0	0%	0	0%	58	4%	210	13%	210	13%	119	7%	1632	100%
loc_9	58	4%	328	20%	346	21%	470	29%	−185	−12%	0	0%	0	0%	0	0%	46	3%	210	13%	210	13%	130	8%	1612	100%
loc_10	58	4%	328	21%	360	23%	369	23%	−354	–22%	0	0%	0	0%	0	0%	47	3%	316	20%	316	20%	138	9%	1576	100%
loc_11	58	4%	328	21%	353	23%	366	23%	−354	–23%	0	0%	0	0%	0	0%	48	3%	316	20%	316	20%	134	9%	1564	100%
loc_12	58	4%	328	21%	350	22%	386	24%	−358	–23%	0	0%	0	0%	0	0%	53	3%	316	20%	316	20%	138	9%	1586	100%
loc_13	58	4%	328	21%	349	22%	386	24%	−358	–23%	0	0%	0	0%	0	0%	51	3%	316	20%	316	20%	138	9%	1583	100%
loc_14	58	4%	328	21%	352	23%	451	29%	−155	−10%	0	0%	0	0%	0	0%	55	4%	316	20%	0	0%	156	10%	1561	100%
loc_15	58	4%	328	21%	348	22%	451	29%	−155	−10%	0	0%	0	0%	0	0%	48	3%	316	20%	0	0%	156	10%	1549	100%
loc_16	58	4%	328	21%	349	22%	397	25%	−360	–23%	0	0%	0	0%	0	0%	50	3%	316	20%	316	20%	143	9%	1595	100%
loc_17	58	4%	328	21%	352	22%	374	24%	−355	–22%	0	0%	0	0%	0	0%	55	3%	316	20%	316	20%	140	9%	1583	100%
loc_18	58	4%	328	21%	344	22%	391	25%	−360	–23%	0	0%	0	0%	0	0%	50	3%	316	20%	316	20%	130	8%	1572	100%
loc_19	58	4%	328	21%	348	22%	371	24%	−354	–23%	0	0%	0	0%	0	0%	50	3%	316	20%	316	20%	140	9%	1571	100%
loc_20	58	4%	328	20%	350	22%	369	23%	−354	–22%	0	0%	0	0%	0	0%	80	5%	316	20%	316	20%	138	9%	1600	100%
loc_21	58	4%	328	21%	347	22%	361	23%	−353	–23%	0	0%	0	0%	0	0%	51	3%	316	20%	316	20%	137	9%	1560	100%
loc_22	58	4%	328	20%	351	21%	475	29%	−186	−11%	0	0%	0	0%	0	0%	50	3%	210	13%	210	13%	136	8%	1633	100%
loc_23	58	4%	328	20%	345	21%	488	30%	−190	−12%	0	0%	0	0%	0	0%	61	4%	210	13%	210	13%	119	7%	1629	100%
loc_24	58	4%	328	20%	357	22%	474	29%	−186	−12%	0	0%	0	0%	0	0%	45	3%	210	13%	210	13%	124	8%	1620	100%
loc_25	58	4%	328	21%	346	22%	470	30%	−161	−10%	0	0%	0	0%	0	0%	46	3%	316	20%	2	0%	144	9%	1549	100%
loc_26	58	4%	328	21%	358	23%	451	29%	−165	−11%	0	0%	0	0%	0	0%	45	3%	316	20%	15	1%	149	10%	1555	100%
loc_27	58	4%	328	21%	350	22%	463	29%	−158	−10%	0	0%	0	0%	0	0%	79	5%	316	20%	0	0%	150	9%	1585	100%
loc_28	58	4%	328	21%	348	22%	481	31%	−163	−11%	0	0%	0	0%	0	0%	49	3%	316	20%	0	0%	133	9%	1550	100%
loc_29	70	4%	400	23%	403	23%	496	28%	−122	−7%	0	0%	0	0%	0	0%	47	3%	210	12%	120	7%	134	8%	1759	100%
loc_30	70	4%	400	23%	410	23%	481	27%	−125	−7%	0	0%	0	0%	0	0%	52	3%	210	12%	131	7%	143	8%	1772	100%
loc_31	90	4%	521	26%	489	24%	493	24%	−190	−9%	0	0%	0	0%	0	0%	82	4%	210	10%	210	10%	130	6%	2035	100%
loc_32	90	4%	521	26%	487	24%	467	23%	−185	−9%	0	0%	0	0%	0	0%	81	4%	210	10%	210	10%	128	6%	2010	100%
loc_33	90	4%	521	25%	492	24%	500	24%	−193	−9%	0	0%	0	0%	0	0%	133	6%	210	10%	210	10%	109	5%	2072	100%
loc_34	58	4%	328	21%	346	22%	397	25%	−360	–23%	0	0%	0	0%	0	0%	49	3%	316	20%	316	20%	143	9%	1592	100%
loc_35	58	4%	328	21%	350	22%	397	25%	−360	–23%	0	0%	0	0%	0	0%	52	3%	316	20%	316	20%	143	9%	1599	100%
loc_37	220	3%	1341	20%	1268	19%	2402	37%	–223	−3%	0	0%	0	0%	0	0%	197	3%	837	13%	0	0%	502	8%	6544	100%
loc_38	221	3%	1340	20%	1278	19%	2404	36%	–223	−3%	0	0%	0	0%	0	0%	222	3%	837	13%	0	0%	520	8%	6600	100%
loc_39	311	3%	1927	19%	1853	19%	4415	44%	−118	−1%	0	0%	0	0%	0	0%	174	2%	837	8%	0	0%	591	6%	9991	100%
loc_40	220	3%	1341	20%	1269	19%	2411	37%	−224	−3%	0	0%	0	0%	0	0%	187	3%	837	13%	0	0%	523	8%	6565	100%
loc_41	311	3%	1927	19%	1857	19%	4431	44%	−121	−1%	0	0%	0	0%	0	0%	176	2%	837	8%	0	0%	593	6%	10,011	100%
loc_42	220	3%	1341	20%	1277	19%	2415	37%	−225	−3%	0	0%	0	0%	0	0%	195	3%	837	13%	0	0%	516	8%	6577	100%
loc_43	311	3%	1927	19%	1850	19%	4430	44%	−122	−1%	0	0%	0	0%	0	0%	174	2%	837	8%	0	0%	576	6%	9983	100%
loc_44	221	3%	1341	20%	1315	20%	2404	36%	–222	−3%	0	0%	0	0%	0	0%	154	2%	837	13%	0	0%	546	8%	6597	100%
loc_45	221	3%	1340	20%	1279	20%	2408	37%	−224	−3%	0	0%	0	0%	0	0%	167	3%	837	13%	0	0%	521	8%	6548	100%
loc_46	1132	6%	1169	6%	0	0%	12,758	68%	−91	0%	0	0%	1919	10%	610	3%	184	1%	837	4%	0	0%	134	1%	18,652	100%
loc_47	990	3%	1891	7%	0	0%	22,333	77%	–23	0%	0	0%	1919	7%	793	3%	339	1%	837	3%	0	0%	0	0%	29,080	100%
loc_48	220	3%	1341	20%	1283	20%	2411	37%	−225	−3%	0	0%	0	0%	0	0%	204	3%	837	13%	0	0%	506	8%	6578	100%
loc_49	221	3%	1341	20%	1285	19%	2425	37%	−227	−3%	0	0%	0	0%	0	0%	189	3%	837	13%	0	0%	522	8%	6592	100%
loc_50	465	4%	830	7%	0	0%	8950	71%	−100	−1%	563	4%	0	0%	531	4%	173	1%	837	7%	0	0%	283	2%	12,533	100%
loc_51	820	3%	1180	5%	0	0%	17,801	76%	−46	0%	0	0%	1919	8%	689	3%	293	1%	837	4%	0	0%	26	0%	23,519	100%

A.6. Analysis for the terraced houses

Fig. 17 depicts the cost-dependent decisions of the consumer at location10, a semi-detached house. The design decisions of this house are in line with the majority of the semi-detached and terraced houses. Here, it can be seen that the cost-optimal layout relies on high-temperature district heat for domestic hot water and low-temperature heat for floor heating from the 5GDHC network for low-temperature heat prices up to15 ct/kWh and completely on high-temperature district heat for both, domestic hot water and radiator heating at prices of 20 ct/kWh for low-temperature heat. In particular, this means that the cost-optimal solution for the consumer at location 10 never comprises a heat pump of any kind due to his small energy demands and the relatively high offset costs of heat pumps, i.e. their economies of scale.

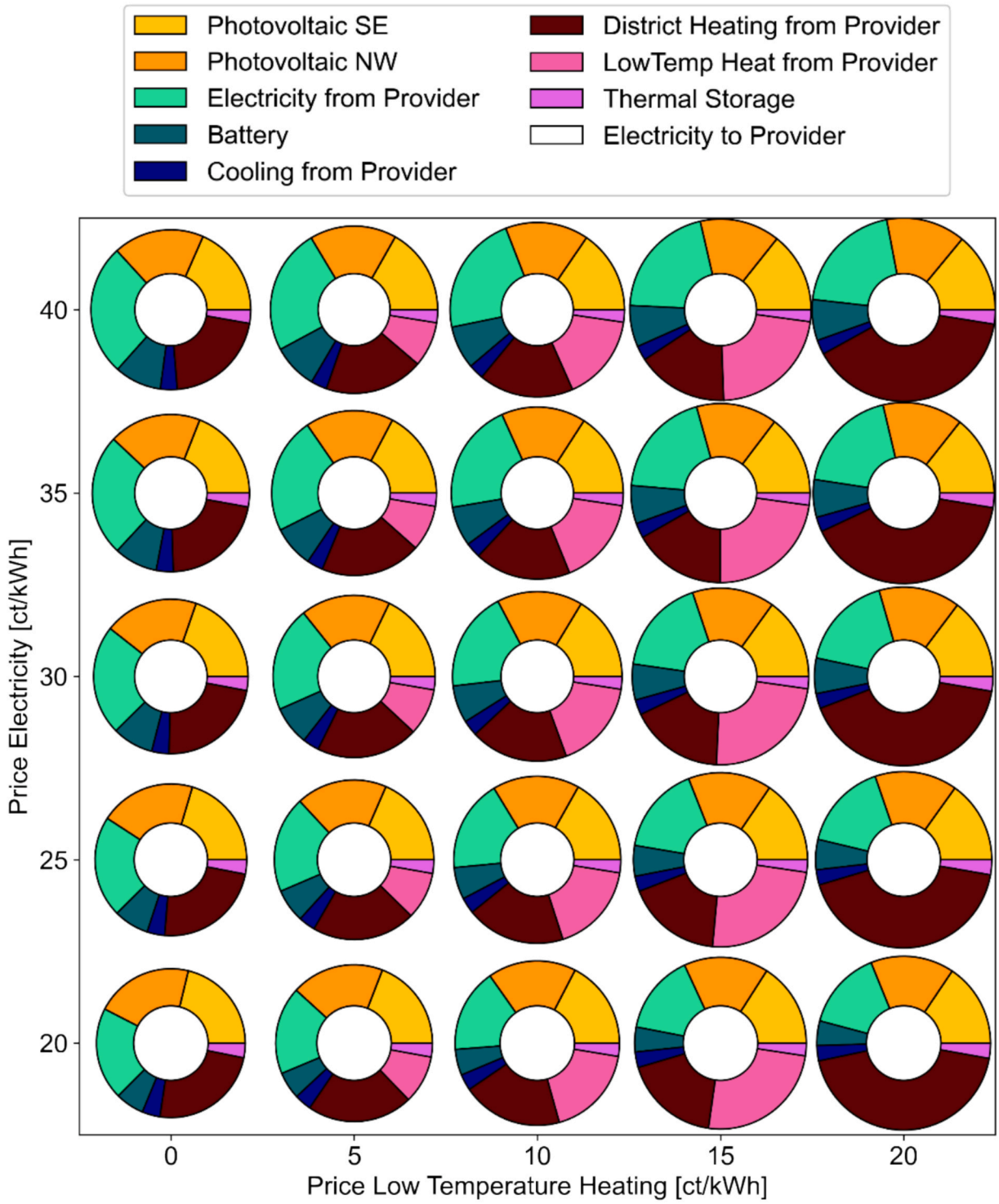

Fig. 17. Price-sensitivity of investment decisions for the building at location 10.

Analogously to the pie charts in Fig. 17, the cash flows for low-temperature heat and electricity increase monotonously for rising respective prices as shown in Fig. 18. Yet, the cash flow for low-temperature heat completely breaks down for prices beyond 16 ct/kWh as it is exchanged for high-

temperature district heating for higher prices. Besides, it can be observed that the absolute cash flow for electricity fed into the grid from photovoltaics is decreasing for rising electricity prices, which emphasizes that the self-consumption rate is increased in order to save costs from electricity purchase.

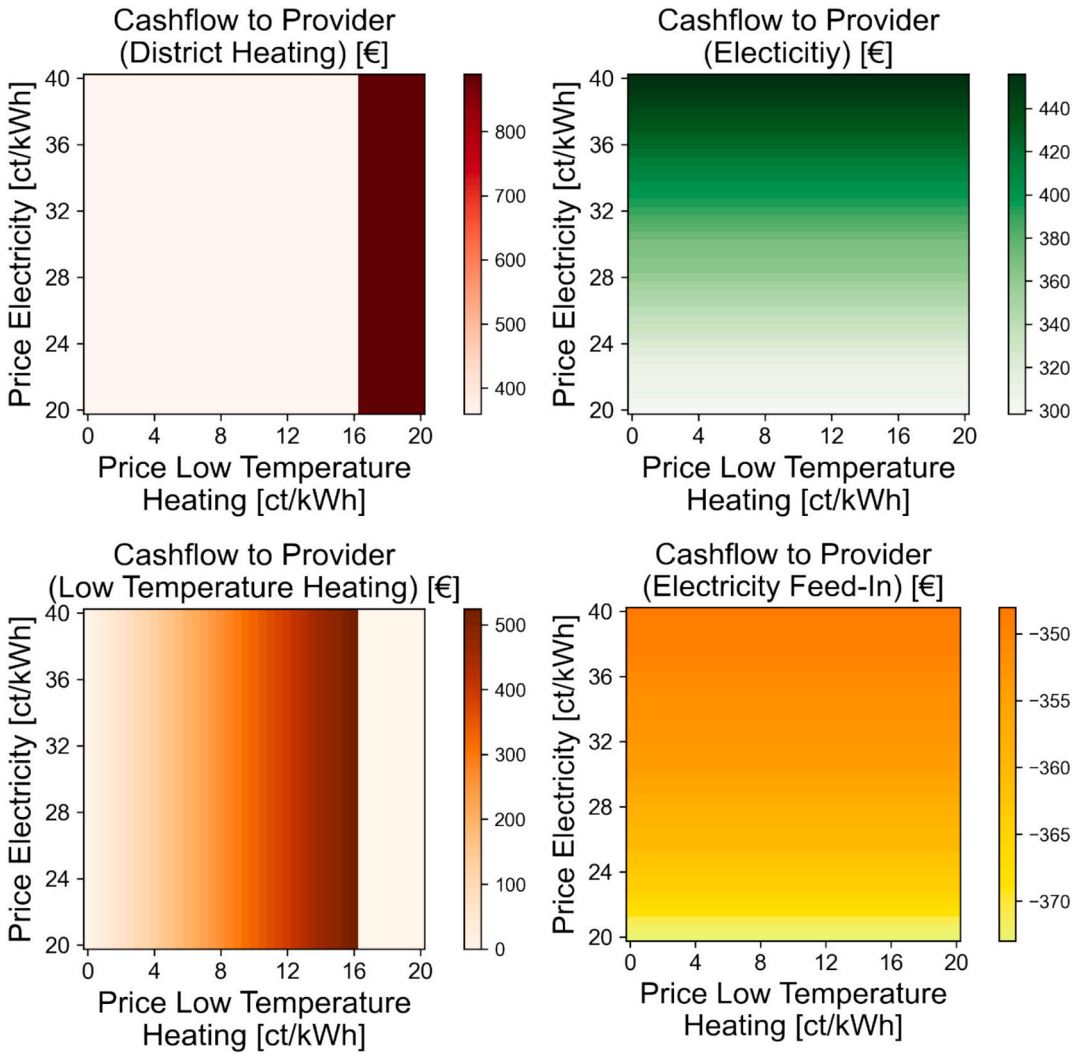

Fig. 18. Cash flows by commodity depending on the price constellation of electricity and low temperature heat for the building at location 10.

Data availability

Data will be made available on request.

References

[1] Grubb, M., C. Vrolijk, and D. Brack, Routledge Revivals: Kyoto Protocol (1999): A Guide and Assessment. 2018: Routledge.

[2] Paris Agreement. Paris agreement. in Report of the Conference of the Parties to the United Nations Framework Convention on Climate Change (21st Session, 2015: Paris). Retrived December. 2015. HeinOnline.

[3] Nolting L, Praktiknjo A. The complexity dilemma – insights from security of electricity supply assessments. Energy 2022;241:122522. https://doi.org/10.1016/j.enpol.2019.06.027.

[4] Kotzur L, et al. A modeler's guide to handle complexity in energy systems optimization. Adv Appl Energy 2021;4:100063. https://doi.org/10.1016/j.adapen.2021.100063.

[5] Wirtz M, et al. Bidirectional low temperature networks in urban districts: a novel design methodology based on mathematical optimization. J Phys Conf Ser 2019;1343(1):012111. https://doi.org/10.1088/1742-6596/1343/1/012111.

[6] Wirtz M, et al. 5th generation district heating: a novel design approach based on mathematical optimization. Appl Energy 2020;260:114158. https://doi.org/10.1016/j.apenergy.2019.114158.

[7] Wirtz M, et al. Design optimization of multi-energy systems using mixed-integer linear programming: which model complexity and level of detail is sufficient? Energ Conver Manage 2021;240:114249. https://doi.org/10.1016/j.enconman.2021.114249.

[8] Knosala K, et al. Hybrid hydrogen home storage for decentralized energy autonomy. Int J Hydrogen Energy 2021;46(42):21748–63. https://doi.org/10.1016/j.ijhydene.2021.04.036.

[9] Knosala K, et al. The role of hydrogen in German residential buildings. Energ Buildings 2022;276:112480. https://doi.org/10.1016/j.enbuild.2022.112480.

[10] Cerniauskas, S., et al., Wissenschaftliche Begleitstudie der Wasserstoff Roadmap Nordrhein-Westfalen. 2021: Technoökonomische Systemanalyse.

[11] Samsatli S, Staffell I, Samsatli NJ. Optimal design and operation of integrated wind-hydrogen-electricity networks for decarbonising the domestic transport sector in Great Britain. Int J Hydrogen Energy 2016;41(1):447–75. https://doi.org/10.1016/j.ijhydene.2015.10.032.

[12] Welder L, et al. Spatio-temporal optimization of a future energy system for power-to-hydrogen applications in Germany. Energy 2018;158:1130–49. https://doi.org/10.1016/j.energy.2018.05.059.

[13] Stolten, D., et al., Neue Ziele auf alten Wegen? Strategien für eine treibhausgasneutrale Energieversorgung bis zum Jahr 2045. Schriften des Forschungszentrums Jülich Reihe Energie & Umwelt / Energy & Environment. Vol. 577. 2022, Jülich: Forschungszentrum Jülich GmbH Zentralbibliothek, Verlag. VI, 81.

[14] Caglayan DG, et al. Robust design of a future 100% renewable european energy supply system with hydrogen infrastructure. Int J Hydrogen Energy 2021;46(57):29376–90. https://doi.org/10.1016/j.ijhydene.2020.12.197.

[15] Simoes S, et al. The jrc-eu-times model. Assessing the Long-Term Role of the SET Plan Energy Technologies 2013. https://doi.org/10.2790/97596.

[16] Schöb, T., et al. Hydrogen and Heat Storages as Flexibility Sources for a Greenhouse Gas-Neutral German Energy System. 2023.
[17] Jacob R, et al. The future role of thermal energy storage in 100% renewable electricity systems. Renewable Sustainable Energy Transition 2023;4:100059. https://doi.org/10.1016/j.rset.2023.100059.
[18] Behrens J, et al. Reviewing the complexity of endogenous technological learning for energy system modeling. Adv Appl Energy 2024;16:100192. https://doi.org/10.1016/j.adapen.2024.100192.
[19] Persson U, Münster M. Current and future prospects for heat recovery from waste in European district heating systems: a literature and data review. Energy 2016;110:116–28. https://doi.org/10.1016/j.energy.2015.12.074.
[20] Weinand JM, et al. Global LCOEs of decentralized off-grid renewable energy systems. Renew Sustain Energy Rev 2023;183:113478. https://doi.org/10.1016/j.rser.2023.113478.
[21] Wirtz M, et al. Quantifying demand balancing in bidirectional low temperature networks. Energ Buildings 2020;224:110245. https://doi.org/10.1016/j.enbuild.2020.110245.
[22] Boesten S, et al. 5th generation district heating and cooling systems as a solution for renewable urban thermal energy supply. Adv Geosci 2019;49:129–36. https://doi.org/10.5194/adgeo-49-129-2019.
[23] Buffa S, et al. 5th generation district heating and cooling systems: a review of existing cases in Europe. Renew Sustain Energy Rev 2019;104:504–22. https://doi.org/10.1016/j.rser.2018.12.059.
[24] Huang P, et al. A review of data centers as prosumers in district energy systems: renewable energy integration and waste heat reuse for district heating. Appl Energy 2020;258:114109. https://doi.org/10.1016/j.apenergy.2019.114109.
[25] Brange L, Englund J, Lauenburg P. Prosumers in district heating networks – a Swedish case study. Appl Energy 2016;164:492–500. https://doi.org/10.1016/j.apenergy.2015.12.020.
[26] Wirtz, M. 5th Generation District Heating and Cooling. 2023 [cited May 29, 2025]; Available from: https://www.mwirtz.com/5gdhc.html.
[27] Abugabbara M, et al. Comparative study and validation of a new analytical method for hydraulic modelling of bidirectional low temperature networks. Energy 2024;296:131168. https://doi.org/10.1016/j.energy.2024.131168.
[28] Dibos S, Pesch T, Benigni A. HeatNetSim: an open-source simulation tool for heating and cooling networks suitable for future energy systems. Energy 2024;312:133588. https://doi.org/10.1016/j.energy.2024.133588.
[29] Zhou, Y., et al. Performance Analysis and Operation Optimization of Energy Bus System for Residential Community in the Downstream of Yangtze River. in Proceedings of the 5th International Conference on Building Energy and Environment. 2023. Singapore: Springer Nature Singapore.
[30] Bilardo M, et al. Modelling a fifth-generation bidirectional low temperature district heating and cooling (5GDHC) network for nearly Zero Energy District (nZED). Energy Rep 2021;7:8390–405. https://doi.org/10.1016/j.egyr.2021.04.054.
[31] Zarin Pass R, Wetter M, Piette MA. A thermodynamic analysis of a novel bidirectional district heating and cooling network. Energy 2018;144:20–30. https://doi.org/10.1016/j.energy.2017.11.122.
[32] Bünning F, et al. Bidirectional low temperature district energy systems with agent-based control: Performance comparison and operation optimization. Appl Energy 2018;209:502–15. https://doi.org/10.1016/j.apenergy.2017.10.072.
[33] Prasanna A, Dorer V, Vetterli N. Optimisation of a district energy system with a low temperature network. Energy 2017;137:632–48. https://doi.org/10.1016/j.energy.2017.03.137.
[34] Lagoeiro, H., et al. Feasibility Assessment Tool for District Heating and Cooling (FAST DHC): A Simple Decision Support Tool for the Techno-Economic Evaluation of DHC Networks. in Proceedings of the 19th International Symposium on District Heating and Cooling. 2026. Cham: Springer Nature Switzerland.
[35] Etemad A, et al. A techno-economic assessment framework for district-scale thermal source networks serving existing buildings. Energ Buildings 2025;338:115737. https://doi.org/10.1016/j.enbuild.2025.115737.
[36] Etemad A, et al. Evaluating the impact of thermal energy storage on grid flexibility in district thermal source networks. J Phys Conf Ser 2025;3140(6):062003. https://doi.org/10.1088/1742-6596/3140/6/062003.
[37] Müller S, et al. Implementation of an expanding thermal source network as a step towards CO2-neutral industry. Energy 2025;330:136766. https://doi.org/10.1016/j.energy.2025.136766.
[38] IEA DHC. District heating network generation definitions 2024 [cited February 21, 2026]; Available from: https://www.iea-dhc.org/fileadmin/public_documents/2402_IEA_DHC_DH_generations_definitions.pdf.
[39] Lund, H., et al., Book of Abstracts, in 10th International Conference on Smart Energy Systems. 2024, Aalborg Universitet. p. 2-3.
[40] Pellegrini M, Bianchini A. The innovative concept of cold district heating networks: a literature review. Energies 2018;11(1). https://doi.org/10.3390/en11010236.
[41] Stubler, A., D. Bestenlehner, and H. Druck. Energy saving potentials of cold district heating networks. in Proceedings of the 17th EWA Symposium during IFAT. 2014.
[42] Francesca, B., et al., MILP based approach for the preliminary investigation of thermal networks in urban areas, in Proceedings of Building Simulation 2021: 17th Conference of IBPSA. 2021, IBPSA. p. 581-588. DOI: https://doi.org/10.26868/25222708.2021.30901.
[43] Gabrielli P, et al. Optimization of low-carbon multi-energy systems with seasonal geothermal energy storage: the Anergy Grid of ETH Zurich. Energy Convers Manage: X 2020;8:100052. https://doi.org/10.1016/j.ecmx.2020.100052.
[44] Zach F, Kretschmer F, Stoeglehner G. Integrating energy demand and local renewable energy sources in smart urban development zones: new options for climate-friendly resilient urban planning. Energies 2019;12(19):3672. https://doi.org/10.3390/en12193672.
[45] Song WH, et al. Modelling development and analysis on the Balanced Energy Networks (BEN) in London. Appl Energy 2019;233–234:114–25. https://doi.org/10.1016/j.apenergy.2018.10.054.
[46] Quirosa G, et al. Energy analysis of an ultra-low temperature district heating and cooling system with coaxial borehole heat exchangers. Energy 2023;278:127885. https://doi.org/10.1016/j.energy.2023.127885.
[47] Quirosa G, et al. Energetic and economic analysis of decoupled strategy for heating and cooling production with CO2 booster heat pumps for ultra-low temperature district network. Journal of Building Engineering 2022;45:103538. https://doi.org/10.1016/j.jobe.2021.103538.
[48] Sommer T, et al. The reservoir network: a new network topology for district heating and cooling. Energy 2020;199:117418. https://doi.org/10.1016/j.energy.2020.117418.
[49] Sommer T, Mennel S, Sulzer M. Lowering the pressure in district heating and cooling networks by alternating the connection of the expansion vessel. Energy 2019;172:991–6. https://doi.org/10.1016/j.energy.2019.02.010.
[50] Ruesch F, Haller M. Potential and limitations of using low-temperature district heating and cooling networks for direct cooling of buildings. Energy Procedia 2017;122:1099–104. https://doi.org/10.1016/j.egypro.2017.07.443.
[51] Chicherin S. Top-down GIS-driven method for configuring the network layout of a 5th generation district heating and cooling (5GDHC) system. Energy 2025;328:136639. https://doi.org/10.1016/j.energy.2025.136639.
[52] Gjoka K, Rismanchi B, Crawford RH. Towards sustainable urban energy solutions: a multi-dimensional assessment framework for fifth-generation district heating and cooling systems. Energ Buildings 2025;326:115071. https://doi.org/10.1016/j.enbuild.2024.115071.
[53] Hachez J, et al. Multi-energy systems fast optimization: a new formulation in linear programming for temperatures and magnitudes of thermal power flows in heating systems. Energ Buildings 2025;336:115618. https://doi.org/10.1016/j.enbuild.2025.115618.
[54] Boussaid T, et al. Enabling fast prediction of district heating networks transients via a physics-guided graph neural network. Appl Energy 2024;370:123634. https://doi.org/10.1016/j.apenergy.2024.123634.
[55] Chaudhry AM, et al. Improving the potential of fifth-generation district heating and cooling networks through robust design and operational optimization under future energy market and demand uncertainties. Energ Buildings 2024;325:114998. https://doi.org/10.1016/j.enbuild.2024.114998.
[56] Soleimani S, et al. Optimal operation of a district heating system using a PV-assisted CO2 heat pump and thermal energy storage. ASME 2024 18th International Conference on Energy Sustainability Collocated with the ASME 2024 Heat Transfer Summer Conference and the ASME 2024 Fluids Engineering Division Summer Meeting. 2024.
[57] Zhang Y, et al. Temperature control strategies for fifth generation district heating and cooling systems: a review and case study. Appl Energy 2024;376:124156. https://doi.org/10.1016/j.apenergy.2024.124156.
[58] Abugabbara M, et al. How to develop fifth-generation district heating and cooling in Sweden? Application review and best practices proposed by middle agents. Energy Rep 2023;9:4971–83. https://doi.org/10.1016/j.egyr.2023.04.048.
[59] Bu T, et al. Design and operation investigation for the fifth-generation heating and cooling system based on load forecasting in business districts. Energ Buildings 2023;294:113243. https://doi.org/10.1016/j.enbuild.2023.113243.
[60] Buonomano A, et al. Solar-assisted district heating networks: Development and experimental validation of a novel simulation tool for the energy optimization. Energ Conver Manage 2023;288:117133. https://doi.org/10.1016/j.enconman.2023.117133.
[61] Qin Q, Gosselin L. Community-based transactive energy market concept for 5th generation district heating and cooling through distributed optimization. Appl Energy 2024;371:123666. https://doi.org/10.1016/j.apenergy.2024.123666.
[62] Qin, Q. and L. Gosselin. Economic Assessment of Bidirectional Low-Temperature District Energy Systems with Seasonal Energy Storage and Photovoltaic Thermal Hybrid Solar System. in Proceedings of the 5th International Conference on Building Energy and Environment. 2023. Singapore: Springer Nature Singapore.
[63] Wirtz M. nPro: a web-based planning tool for designing district energy systems and thermal networks. Energy 2023;268:126575. https://doi.org/10.1016/j.energy.2022.126575.
[64] Wirtz M, et al. Multi-period design optimization for a 5th generation district heating and cooling network. Energ Buildings 2023;284:112858. https://doi.org/10.1016/j.enbuild.2023.112858.
[65] Wirtz M, et al. 5th generation district heating and cooling network planning: a Dantzig–Wolfe decomposition approach. Energ Conver Manage 2023;276:116593. https://doi.org/10.1016/j.enconman.2022.116593.
[66] Zhang Y, Johansson P, Kalagasidis AS. Roadmaps for heating and cooling system transitions seen through uncertainty and sensitivity analysis. Energ Conver Manage 2023;292:117422. https://doi.org/10.1016/j.enconman.2023.117422.
[67] Calise F, et al. Optimal design of a 5th generation district heating and cooling network based on seawater heat pumps. Energ Conver Manage 2022;267:115912. https://doi.org/10.1016/j.enconman.2022.115912.
[68] Meibodi SS, Loveridge F. The future role of energy geostructures in fifth generation district heating and cooling networks. Energy 2022;240:122481. https://doi.org/10.1016/j.energy.2021.122481.

[69] Edtmayer H, et al. Investigation on sector coupling potentials of a 5th generation district heating and cooling network. Energy 2021;230:120836. https://doi.org/10.1016/j.energy.2021.120836.

[70] Hering D, Xhonneux A, Müller D. Design optimization of a heating network with multiple heat pumps using mixed integer quadratically constrained programming. Energy 2021;226:120384. https://doi.org/10.1016/j.energy.2021.120384.

[71] Lund H, et al. Perspectives on fourth and fifth generation district heating. Energy 2021;227:120520. https://doi.org/10.1016/j.energy.2021.120520.

[72] Reiners T, et al. Heat pump efficiency in fifth generation ultra-low temperature district heating networks using a wastewater heat source. Energy 2021;236:121318. https://doi.org/10.1016/j.energy.2021.121318.

[73] Wirtz M, et al. Temperature control in 5th generation district heating and cooling networks: an MILP-based operation optimization. Appl Energy 2021;288:116608. https://doi.org/10.1016/j.apenergy.2021.116608.

[74] Abugabbara M, et al. Bibliographic analysis of the recent advancements in modeling and co-simulating the fifth-generation district heating and cooling systems. Energ Buildings 2020;224:110260. https://doi.org/10.1016/j.enbuild.2020.110260.

[75] Buffa S, et al. Fifth-generation district heating and cooling substations: demand response with artificial neural network-based model predictive control. Energies 2020;13(17):4339. https://doi.org/10.3390/en13174339.

[76] Revesz A, et al. Developing novel 5th generation district energy networks. Energy 2020;201:117389. https://doi.org/10.1016/j.energy.2020.117389.

[77] von Rhein J, et al. Development of a topology analysis tool for fifth-generation district heating and cooling networks. Energ Conver Manage 2019;196:705–16. https://doi.org/10.1016/j.enconman.2019.05.066.

[78] Dempe, S., et al., Bilevel Programming Problems: Theory, Algorithms and Applications to Energy Networks. 1 ed. Energy Systems. 2015, Heidelberg: Springer Berlin. XII, 325.

[79] Von Stackelberg, H., Marktform und Gleichgewicht. 1934: J. springer.

[80] Luo, Z.-Q., J.-S. Pang, and D. Ralph, Mathematical programs with equilibrium constraints. 1996: Cambridge University Press.

[81] Fortuny-Amat J, McCarl B. A representation and economic interpretation of a two-level programming problem. J Oper Res Soc 1981;32(9):783–92. https://doi.org/10.1057/jors.1981.156.

[82] Li R, et al. Participation of an energy hub in electricity and heat distribution markets: an MPEC approach. IEEE Trans Smart Grid 2019;10(4):3641–53. https://doi.org/10.1109/TSG.2018.2833279.

[83] Li G, et al. Security-constrained bi-level economic dispatch model for integrated natural gas and electricity systems considering wind power and power-to-gas process. Appl Energy 2017;194:696–704. https://doi.org/10.1016/j.apenergy.2016.07.077.

[84] Hu Z, et al. Bi-level robust dynamic economic emission dispatch considering wind power uncertainty. Electr Pow Syst Res 2016;135:35–47. https://doi.org/10.1016/j.epsr.2016.03.010.

[85] Ju L, et al. A bi-level stochastic scheduling optimization model for a virtual power plant connected to a wind–photovoltaic–energy storage system considering the uncertainty and demand response. Appl Energy 2016;171:184–99. https://doi.org/10.1016/j.apenergy.2016.03.020.

[86] Škugor B, Deur J. A bi-level optimisation framework for electric vehicle fleet charging management. Appl Energy 2016;184:1332–42. https://doi.org/10.1016/j.apenergy.2016.03.091.

[87] Feijoo F, Das TK. Emissions control via carbon policies and microgrid generation: a bilevel model and Pareto analysis. Energy 2015;90:1545–55. https://doi.org/10.1016/j.energy.2015.06.110.

[88] Liu J, Li J. A bi-level energy-saving dispatch in smart grid considering interaction between generation and load. IEEE Trans Smart Grid 2015;6(3):1443–52. https://doi.org/10.1109/TSG.2014.2386780.

[89] Valinejad J, Barforoushi T. Generation expansion planning in electricity markets: a novel framework based on dynamic stochastic MPEC. Int J Electr Power Energy Syst 2015;70:108–17. https://doi.org/10.1016/j.ijepes.2015.02.002.

[90] Jenabi M, Ghomi SMTF, Smeers Y. Bi-level game approaches for coordination of generation and transmission expansion planning within a market environment. IEEE Trans Power Syst 2013;28(3):2639–50. https://doi.org/10.1109/TPWRS.2012.2236110.

[91] Pina EA, Lozano MA, Serra LM. Assessing the influence of legal constraints on the integration of renewable energy technologies in polygeneration systems for buildings. Renew Sustain Energy Rev 2021;149:111382. https://doi.org/10.1016/j.rser.2021.111382.

[92] Koirala BP, et al. Energetic communities for community energy: a review of key issues and trends shaping integrated community energy systems. Renew Sustain Energy Rev 2016;56:722–44. https://doi.org/10.1016/j.rser.2015.11.080.

[93] Billerbeck A, et al. Policy frameworks for district heating: a comprehensive overview and analysis of regulations and support measures across Europe. Energ Policy 2023;173:113377. https://doi.org/10.1016/j.enpol.2022.113377.

[94] European Commission, Directive (EU) 2018/2001 of the European Parliament and of the Council of 11 December 2018. 2018, Official Journal of the European Union.

[95] Barabino E, et al. Energy communities: a review on trends, energy system modelling, business models, and optimisation objectives. Sustainable Energy Grids Networks 2023;36:101187. https://doi.org/10.1016/j.segan.2023.101187.

[96] Gianaroli F, et al. Exploring the academic landscape of energy communities in Europe: a systematic literature review. J Clean Prod 2024;451:141932. https://doi.org/10.1016/j.jclepro.2024.141932.

[97] Benalcazar P, Suski A, Kamiński J. The effects of capital and energy subsidies on the optimal design of microgrid systems. Energies 2020;13(4):955. https://doi.org/10.3390/en13040955.

[98] Pinto ES, Serra LM, Lázaro A. Optimization of the design of polygeneration systems for the residential sector under different self-consumption regulations. Int J Energy Res 2020;44(14):11248–73. https://doi.org/10.1002/er.5738.

[99] González-Mahecha RE, et al. Optimization model for evaluating on-site renewable technologies with storage in zero/nearly zero energy buildings. Energ Buildings 2018;172:505–16. https://doi.org/10.1016/j.enbuild.2018.04.027.

[100] Renaldi R, Kiprakis A, Friedrich D. An optimisation framework for thermal energy storage integration in a residential heat pump heating system. Appl Energy 2017;186:520–9. https://doi.org/10.1016/j.apenergy.2016.02.067.

[101] Schütz T, et al. Optimal design of energy conversion units for residential buildings considering German market conditions. Energy 2017;139:895–915. https://doi.org/10.1016/j.energy.2017.08.024.

[102] Harb H, et al. MIP approach for designing heating systems in residential buildings and neighbourhoods. J Build Perform Simul 2016;9(3):316–30. https://doi.org/10.1080/19401493.2015.1051113.

[103] Lozano MA, Ramos JC, Serra LM. Cost optimization of the design of CHCP (combined heat, cooling and power) systems under legal constraints. Energy 2010;35(2):794–805. https://doi.org/10.1016/j.energy.2009.08.022.

[104] Delorme, R., et al., Der deutsche Förderdschungel bremst die Wärmewende im Gebäudesektor Energiewirtschaftliche Tagesfragen, 2022.

[105] Hoffmann, M., F. Borggrefe, and A. Praktiknjo, Regulations and Contract Design in Multi-Agent District Heating and Cooling Systems, in 44th IAEE International Conference. 2023: Riyadh, Saudi Arabia.

[106] Borggrefe, F., et al., Heating in German City Quarters: How does the Regulatory Framework Influence Investments in Renewable Technologies?, in 44th IAEE International Conference. 2023: Riyadh, Saudi Arabia.

[107] Borggrefe, F., et al., Modellierung energiepolitischer Anreize und Hemmnisse für die Wärmewende: Wirtschaftliche potentiale für erneuerbare Nahwärmenetze, in 13. Internationale Energiewirtschaftstagung an der TU Wien (IEWT 2023). 2023: Vienna, Austria.

[108] Tang, C.-F., et al., Einfluss des regulatorischen Rahmens auf Technologieoptionen in energetischen Quartierskonzepten, in 13. Internationale Energiewirtschaftstagung an der TU Wien (IEWT 2023). 2023: Vienna, Austria.

[109] The TransUrban.NRW Consortium, 3. Gesamtzwischenbericht des TransUrban.NRW Projekts. 2022: Unpublished.

[110] European Central Bank. Inflation and Consumer Prices. 2025 [cited November 2, 2025]; Available from: https://www.ecb.europa.eu/stats/macroeconomic_and_sectoral/hicp/html/index.en.html.

[111] KPMG. KPMG Cost of Capital Study. 2025 [cited November 2, 2025]; Available from: https://kpmg.com/de/en/home/insights/overview/cost-of-capital.study.html.

[112] Umweltbundesamt. CO2-Emissionen pro Kilowattstunde Strom steigen 2021 wieder an. 2022 [cited September 20, 2022]; Available from: https://www.umweltbundesamt.de/themen/co2-emissionen-pro-kilowattstunde-strom-steigen.

[113] Hakenes, J. Fernwärme: Technik, Nutzung, Kosten und Alternativen. 2022 [cited September 20, 2022]; Available from: https://www.co2online.de/modernisieren-und-bauen/heizung/fernwaerme/.

[114] Klütz T, et al. ETHOS.FINE: A framework for integrated energy system assessment. Journal of Open Source Software 2025;10(105):6274. https://doi.org/10.21105/joss.06274.

[115] Hoffmann MAC. Temporal aggregation methods for energy system modeling. Jülich: RWTH Aachen University; 2022. DOI: https://doi.org/10.18154/RWTH-2023-06886.

[116] Hoffmann M, Kotzur L, Stolten D. The Pareto-optimal temporal aggregation of energy system models. Appl Energy 2022;315:119029. https://doi.org/10.1016/j.apenergy.2022.119029.

[117] Hoffmann M, et al. Typical periods or typical time steps? A multi-model analysis to determine the optimal temporal aggregation for energy system models. Appl Energy 2021;304:117825. https://doi.org/10.1016/j.apenergy.2021.117825.

[118] Hoffmann M, et al. A review on time series aggregation methods for energy system models. Energies 2020;13(3):641. https://doi.org/10.3390/en13030641.

[119] Kannengießer T, et al. Reducing computational load for mixed integer linear programming: an example for a district and an island energy system. Energies 2019;12(14):2825. https://doi.org/10.3390/en12142825.

[120] Singh B, et al. Budget-cut: introduction to a budget based cutting-plane algorithm for capacity expansion models. Optim Lett 2022;16(5):1373–91. https://doi.org/10.1007/s11590-021-01826-w.

[121] Sinha A, et al. Bilevel optimization based on iterative approximation of multiple mappings. J Heuristics 2020;26(2):151–85. https://doi.org/10.1007/s10732-019-09426-9.

[122] Priesmann J, Praktiknjo A. Estimating short- and long-run price and income elasticities of final energy demand as a function of household income. Energ Policy 2025;207:114850. https://doi.org/10.1016/j.enpol.2025.114850.

[123] Deutscher Bundestag, Gesetz über die Elektrizitäts- und Gasversorgung (Energiewirtschaftsgesetz - EnWG). 2025, Bundesministerium der Justiz und für Verbraucherschutz.

[124] European Commission, Directive (EU) 2023/2413 of the European Parliament and of the Council of 18 October 2023. 2023, Official Journal of the European Union.

[125] Deutscher Bundestag, Gesetz für den Ausbau erneuerbarer Energien (Erneuerbare-Energien-Gesetz - EEG). 2023, Bundesministerium der Justiz und für Verbraucherschutz.

[126] Deutscher Bundestag, Titel: „Energy Sharing“: Regelungen zur gemeinsamen Energieerzeugung, W. Dienste, Editor. 2024, Deutscher Bundestag.
[127] European Commission, Directive (EU) 2019/944 of the European Parliament and of the Council of 5 June 2019. 2019, Official Journal of the European Union.
[128] Bundesversammlung der Schweizerischen Eidgenossenschaft, Energiegesetz, EnG. 2025, Fedlex.
[129] Bundesversammlung der Schweizerischen Eidgenossenschaft, Stromversorgungsgesetz, StromVG. 2025, Fedlex.
[130] Nolting L, Schuller V, Gaumnitz F, Praktiknjo A. Incentivizing timely investments in electrical grids: analysis of the amendment of the German distribution grid regulation. Energ Policy 2019;132(9). https://doi.org/10.1016/j.enpol.2019.06.027.
[131] Maier R, et al. Impact of foresight horizons on energy system decarbonization pathways. Adv Appl Energy 2025;18:100217. https://doi.org/10.1016/j.adapen.2025.100217.
[132] Omoyele O, et al. Impact of temporal resolution on the design and reliability of residential energy systems. Energ Buildings 2024;319:114411. https://doi.org/10.1016/j.enbuild.2024.114411.
[133] Omoyele O, et al. Increasing the resolution of solar and wind time series for energy system modeling: a review. Renew Sustain Energy Rev 2024;189:113792. https://doi.org/10.1016/j.rser.2023.113792.
[134] Mantuano C, et al. Data imputation methods for intermittent renewable energy sources: Implications for energy system modeling. Energ Conver Manage 2025;339:119857. https://doi.org/10.1016/j.enconman.2025.119857.
[135] Omoyele O, et al. A High-Resolution Downscaling Approach for Solar Irradiance using Statistical Parameter Matching. Renew Energ 2026;256:124551. https://doi.org/10.1016/j.renene.2025.124551.
[136] Krampe, L., M. Wünsch, and M. Koepp, Eigenversorgung aus Solaranlagen.: Das Potenzial für Photovoltaik-Speicher-Systeme in Ein-und Zweifamilienhäusern Landwirtschaft sowie im Lebensmittelhandel. 2016.
[137] Mayer, J.N., et al., Current and future cost of photovoltaics. Long-term Scenarios for Market Development, System Prices LCOE of Utility-Scale PV Systems. 2015.
[138] Wolf. Preisliste Heizsysteme. 2016 [cited June 11, 2021]; Available from: https://www.ck-heiztechnik.de/media/kataloge/wolf/Wolf-Preisliste-Heizsysteme-03-2016.pdf.
[139] Lindberg KB, et al. Cost-optimal energy system design in zero energy buildings with resulting grid impact: a case study of a german multi-family house. Energ Buildings 2016;127:830–45. https://doi.org/10.1016/j.enbuild.2016.05.063.
[140] Remmen P, et al. TEASER: an open tool for urban energy modelling of building stocks. J Build Perform Simul 2018;11(1):84–98. https://doi.org/10.1080/19401493.2017.1283539.
[141] Jordan, U. and K. Vajen. DHWcalc: Program to generate domestic hot water profiles with statistical means for user defined conditions. in Proceedings of the ISES Solar World Congress, Orlando, FL, USA. 2005.
[142] Deutscher Wetterdienst, TRY - Testreferenzjahre. 2022.
[143] Kotzur, L., Future Grid Load of the Residential Building Sector, in Schriften des Forschungszentrums Jülich Reihe Energie & Umwelt / Energy & Environment. 2018, RWTH Aachen: Jülich. p. xxi, 213 S. DOI: https://doi.org/10.18154/RWTH-2018-231872.
[144] McKenna E, Thomson M. High-resolution stochastic integrated thermal–electrical domestic demand model. Appl Energy 2016;165:445–61. https://doi.org/10.1016/j.apenergy.2015.12.089.
[145] Hoffmann M, et al. A review of mixed-integer linear formulations for framework-based energy system models. Adv Appl Energy 2024;16:100190. https://doi.org/10.1016/j.adapen.2024.100190.
[146] Samsatli S, Samsatli NJ. A general spatio-temporal model of energy systems with a detailed account of transport and storage. Comput Chem Eng 2015;80:155–76. https://doi.org/10.1016/j.compchemeng.2015.05.019.
[147] oemof Developer Team. oemof.thermal Documentation: Compression heat pump and chiller. 2019 [cited 07.07.2022, 2022]; Available from: https://oemof-thermal.readthedocs.io/en/latest/compression_heat_pumps_and_chillers.html.
[148] Hilpert S, et al. The Open Energy Modelling Framework (oemof)-a new approach to facilitate open science in energy system modelling. Energ Strat Rev 2018;22:16–25.